Chapter 9
Preparation of Functional Peanut Oligopeptide and Its Biological Activity

Biopeptides are peptidic compounds that are beneficial or biologically active to the life activities of living organisms (Liu and Cao 2002; Pang Guangchang et al. 2001). Since Brantl et al. (1979) first reported that small peptide with morphine-like activity was found from the small intestine of guinea pig fed with bovine casein zymolyte, a variety of bioactive peptides have been isolated from the animals, plants, and microorganisms (Gill et al. 1996). Among them, peptides that are composed of two to more than ten amino acids with biological activity are known as functional oligopeptides. Functional oligopeptides belong to biologically active peptides. Modern nutrition studies have found that proteins are not completely absorbed in the form of free amino acids after the action of digestive tract enzymes but are absorbed mainly in the form of oligopeptides; the biological meaning of functional oligopeptides is mainly reflected in both a variety of functional activity and completely independent absorption mechanism.

The peanut protein products on the domestic market mainly include peanut protein powder, and it is mainly used as the basic raw material for food processing. Peanut protein powder has such shortcomings as poor functional properties and biological activity, so peanut protein powder is used as the raw material to make functional peanut oligopeptides to improve the functional characteristics of peanut protein, release the functional peptide fragments in protein, fill the blank in peanut protein processing products in China, and effectively improve the conversion rate and utilization rate of peanut processing. This is of great significance to optimize peanut industry structure and product structure, as well as promote the development peanut protein industry and even functional food industry.

At present, China's soybean protein peptide and milk peptide have achieved industrialization, the production mostly adopts directional enzymatic hydrolysis and controllable proteolysis, microbial fermentation, and other technologies. However, there is a lack of detailed research and optimization for oligopeptide production process and its parameters in China, so that most of the peptide products are crude peptides with low purity and low degree of hydrolysis, and functional

Q. Wang, *Peanut Processing Characteristics and Quality Evaluation*,
DOI 10.1007/978-981-10-6175-2_9

oligopeptide products with high purity and high degree of hydrolysis are lacked; in addition, the raw material selection for oligopeptides with corresponding functional activities remains to be established. Zhang and Wang (2007) optimized compound enzyme method to prepare functional peanut oligopeptides. Wang et al. (2013) isolated and purified peanut oligopeptides and analyzed the structure-function relationship between peanut oligopeptide and its structure. On this basis, Wang et al. (2013) simulated the molecular conformation of peanut oligopeptides with the function to reduce blood pressure using Discovery Studio 3.5 software. These studies provide a theoretical basis for the production, processing, and application of functional peanut oligopeptides in China.

1 Composition of Peanut Oligopeptides

1.1 Basic Components

Functional peanut oligopeptides refer to the peptide matters with relative molecular mass of below 5000 Da that are made from peanut meal or peanut protein by enzymatic hydrolysis or microbial fermentation method. Refer to GB/T 22492–2008 (soybean peptide powder). The sensory quality of peanut peptide powder should meet the requirements of Table 9.1.

Soybean peptides are divided into three levels in GB/T 22492–2008. As the products with high-added value among peanut peptides, the physicochemical indicators of functional peanut oligopeptide should meet the level I standards of soybean peptides (Table 9.2).

1.2 Amino Acid Composition

The analysis results of amino acid showed that the free amino acid content of functional peanut oligopeptides was 66.4 mg/g (Fig. 9.1). It was found that although the hydrolytic degree of compound enzymatic hydrolysis was large, the products were mainly oligopeptides and the content of free amino acids was small.

1.3 Molecular Weight Distribution

The molecular weight distribution of functional peanut oligopeptides was generally analyzed using high-performance liquid chromatography (HPLC). The basic

Table 9.1 Sensory quality of peanut peptide powder

Item	Quality requirements	Item	Quality requirements
Fineness	Pass the sieve with a pore diameter of 0.250 mm by 100%	Taste and smell	Have the special taste and smell of the product, without other smell
Color	White, faint yellow, yellow impurities no visible foreign matter	Impurities	Without visible foreign matters

Table 9.2 Physicochemical indicators of functional peanut oligopeptides

Item	Peanut oligopeptides
Crude protein (calculated by dry basis, $N \times 6.25$)/%	≧90.0
Peptide content (calculated by dry basis)/%	≧80.0
≧Relative molecular mass of 80% peptide fragments/Da	≦2000
Ash (calculated by dry basis)/%	≦6.5
Moisture/%	≦7.0
Crude fat (dry basis)/%	≦1.0
Urease activity	Negative

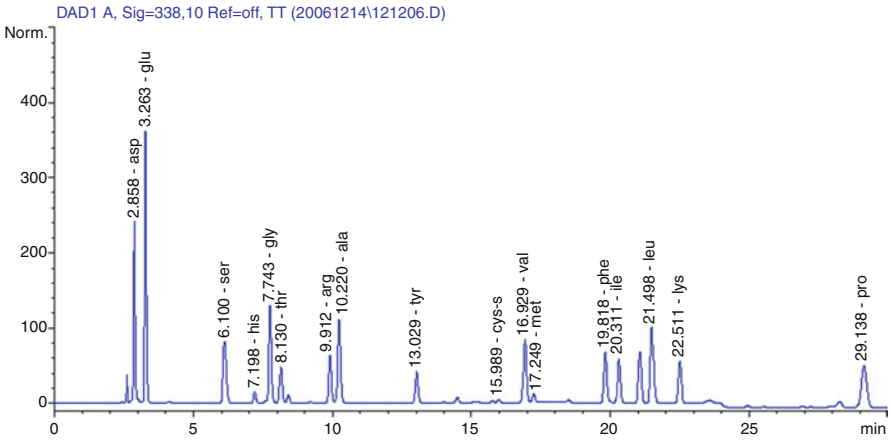

Fig. 9.1 Amino acid composition of functional peanut oligopeptides

conditions are as follows: chromatographic column, TSKgel2000 $_{SWXL}$ 300×7.8 mm; mobile phase, acetonitrile/water/trifluoroacetic acid, 20/80/0.1 (V/V); testing wavelength, 220 nm; flow rate, 0.5 ml/min; testing time, 30 min; and column temperature, room temperature; the molecular weight markers were cytochrome C (M_W12500), bacitracin (M_W1450), aminoethanoic acid-aminoethanoic acid-tyrosine-arginine (M_W451), and aminoethanoic acid-aminoethanoic acid-aminoethanoic acid (M_W189).

When making relative molecular mass standard curve, mobile phase should be used to prepare the above peptide standard solutions with different relative

molecular masses at mass concentration of 1 mg/mL. After mixing it with a certain proportion and filtering it using the organic phase membrane with a pore size of 0.2–0.5 μm, samples were introduced, and then the chromatogram of standard samples was obtained. The retention time was plotted using the logarithm of the relative molecular mass, or linear regression was made to obtain the relative molecular mass correction curves and their equations.

Zhang and Wang (2007) analyzed the molecular weight distribution of functional peanut oligopeptides with cold-pressed peanut meal as raw materials. The regression equation of the standard sample was lgMw = 7.18–0.239T, and the correlation coefficient was $R^2 = 0.9925$, indicating that the relative molecular weight logarithm was well correlated with the elution times of standard samples, and the molecular weight distribution of functional peanut oligopeptides could be tested accurately (Table 9.3). Figure 9.2 was the high-performance liquid chromatogram of volume exclusion of functional peanut oligopeptides. It was shown from the figure that the relative molecular weights of functional peanut oligopeptides were distributed between 126 and 11,197 Da, mainly between 126 and 949 Da.

2 Testing Method of Oligopeptide

2.1 Improvement of Soluble Nitrogen Determination Method

2.1.1 Improvement of Lowry Method

Lowry method means that protein can react with Folin-phenol reagent under alkaline conditions to form copper-protein compound, and then this compound reduces phosphomolybdic acid-phosphotungstic acid reagent producing a dark blue of the molybdenum blue and tungsten blue compound, and such dark blue compound has the maximum absorption peak at 745–750 nm, and the color depth (absorption value) is proportional to the protein concentration (Wang Jiazheng 2002), and the content of protein can be calculated according to the light absorption value at 750 nm. However, the protein concentration and the linear range of absorption value are narrow, being 5–100 μg/ml, because when the protein concentration is greater than 100 μg/ml, the combination rate of protein and copper will decrease with the increase of protein concentration. Therefore, it is required to adjust the protein concentration in the sample to this concentration range during the actual determination; otherwise, a large deviation may be caused to the result. Coakley and James (1978) established a double-reciprocal equation for this case:

Table 9.3 Molecular weight distribution of functional peanut oligopeptides

Retention times of peak values (min)	Relevant molecular weight distribution scope (Da)	Proportion of peak area (%)
13.100–14.933	11,197–4083	2.94
14.933–16.500	4083–1723	3.12
16.500–17.583	1723–949	4.15
17.583–19.050	949–423	20.18
19.050–20.123	423–235	26.49
20.123–21.250	227–126	34.64

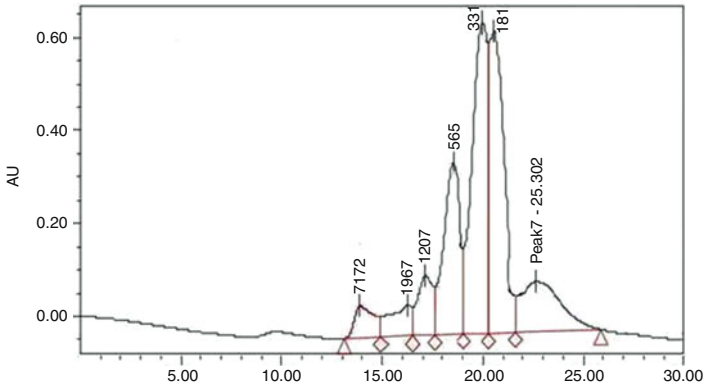

Fig. 9.2 Molecular weight distribution of functional peanut oligopeptide (Standard curve of relative molecular weight: lgMw = 7.18–0.239T, $R = 0.9925$)

$$\frac{1}{A_{750}} = \frac{\Phi}{[P]} + \chi \tag{9.1}$$

This equation can be used to accurately calculate the protein concentration in the sample within the protein concentration range of 0.1–10 mg/ml. The constants can be calculated by two-point method:

$$\Phi = \frac{y_1 - y_2}{x_1 - x_2} \tag{9.2}$$

where $y_1 = \frac{1}{A_{750(1)}}$, $y_2 = \frac{1}{A_{750(2)}}$, $x_1 = \frac{1}{[P]_1}$, and $x_2 = \frac{1}{[P]_2}$

where $[P]$, bovine serum albumin (BSA) concentration, and A_{750}, absorbance of BSA solution with the corresponding concentration at 750 nm:

$$\chi = \bar{y} - \Phi\bar{x} \tag{9.3}$$

where $\bar{y} = \frac{y_1 - y_2}{2}$ and $\bar{x} = \frac{x_1 - x_2}{2}$

Setting $[P]_1 = 0.1$ mg/ml and $[P]_2 = 5$ mg/ml, we obtained $A_{750\,(1)} = 0.254$, $A_{750\,(2)} = 2.728$ by determination.

And $y_1 = 3.937$, $y_2 = 0.3666$, and $\Phi = 0.3643$:

$$\bar{y} = 2.1518, \bar{x} = 5.1, \chi = 0.2939.$$

When the protein content in the sample was within the range of 0.1–10 mg/ml:

$$\frac{1}{A_{750}} = \frac{0.3643}{[P]} + 0.2939 \tag{9.4}$$

When the protein content in sample was within the range of 5–100 μg/ml/ml, a standard curve was established (Fig. 9.3):

Therefore, through the segmentation function, the protein concentration could be calculated when the protein content in the sample was within the range of 5–10 mg/ml. When the absorbance was less than 0.254, the linear equation was used; when the absorbance was more than 0.254, the double-reciprocal equation was adopted.

2.1.2 Verification of Improved Lowry Method

The linearity and double-reciprocal equations were used to calculate the protein content of BSA solution when the concentration was within the range of 120–200 mg/ml. The results are shown in Table 9.4. The recovery rate was always about 100%. It was shown that the double-reciprocal equation could be applied to the determination of protein concentration in the sample with a protein content of 0.1–10 mg/ml.

2.2 Yield of Oligopeptides

In the preparation of oligopeptides, yield was one of the most important evaluation indicators. The yield of oligopeptides was usually determined by trichloroacetic acid precipitation method. That is, first mix the trichloroacetic acid with a concentration of 20% with aqueous solution in 1:1, precipitate macromolecular protein, obtain the supernatant by centrifugation, and then determine soluble protein nitrogen and calculate the yield.

The determination methods of soluble nitrogen usually include Coomassie brilliant blue method, biuret method, Folin-phenol method, and so on. Coomassie brilliant blue method is the most accurate method in the determination of soluble nitrogen. The principle is that Coomassie brilliant blue G-250 can combine with protein in the acidic solution, and thus the maximum absorption peak position of the dye will become 595 nm from 465 nm, and the color of the solution becomes blue from brownish black. The absorbance value determined at 595 nm is proportional to

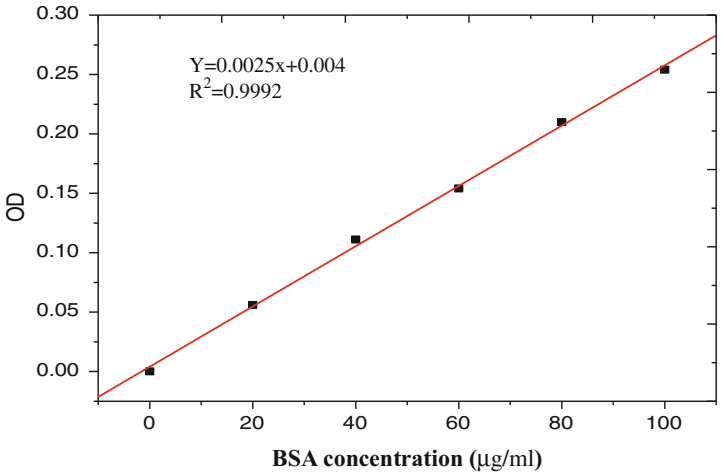

Fig. 9.3 Standard curve by Lowry method

Table 9.4 Verification of improved Lowry method

Actual concentration (mg/ml)	Linear equation (mg/ml)	Recovery rate (%)	Double-reciprocal equation (mg/ml)	Recovery rate (%)
120	120.4 ± 3.61	100.33	122.1 ± 1.32	101.75
140	135.2 ± 2.77	96.57	138.5 ± 2.84	98.93
160	150.8 ± 2.34	94.25	158.3 ± 3.17	98.94
180	168.2 ± 3.19	93.4	183.61 ± 1.71	102.00
200	186.4 ± 1.95	93.20	198.6 ± 2.43	99.30

the protein concentration. However, Coomassie brilliant blue is not suitable for the determination of small-molecule peptide, because the small-molecule peptide cannot be effectively combined with Coomassie brilliant blue G-250 effectively, thus resulting in greater error. The principle of the biuret method is that the biuret is combined with the copper ions in the alkaline solution to form a purple complex. The peptide bonds of protein and polypeptide are similar with the structure of biuret, and they can form purple complex with Cu^{2+}, and its maximum light absorption is at 540 nm. Its color depth is proportional to the protein concentration. But the determination accuracy of biuret method is poor, so it does not apply to accurate quantitative experiments. The principle of Folin-phenol method is to form copper-protein compound using the reaction of protein with Folin-phenol reagent under alkaline condition, and then this compound can reduce phosphomolybdic acid-phosphotungstic acid reagent to produce the dark blue molybdenum blue and tungsten blue compound. Such dark blue compound has the maximum absorption peak at 745–750 nm, the color depth (absorbance) is proportional to the protein concentration, and the protein content can be calculated according to the light

absorption value at 750 nm. The method can be used to accurately determine small-molecule proteins and polypeptides and is more suitable for the determination of polypeptide yield.

2.3 Degree of Hydrolysis

DH (degree of hydrolysis) represents the degree or percentage of peptide bond breakage in protein during the hydrolysis process. The mathematical expression is:

$$DH = \frac{h}{h_{hot}} \times 100\% \tag{9.5}$$

where h is the number of peptide bonds broken, h_{tot} is the total number of peptide bonds in the protein, and h and h_{tot} are often expressed in mmol/g. For a particular protein, h_{tot} is a constant, and it can be calculated according to the components of amino acids in the protein. h_{tot} of peanut protein is about 7.13 mmol/g.

In the hydrolysis process, when the peptide bond is broken, new –COOH and –NH will be formed, so the number of hydrolyzed peptide bonds can be determined by measuring the number of newly formed terminal –COOH or –NH groups after hydrolysis.

Commonly used methods for the determination of degree of hydrolysis include pH-stat method, trinitrobenzene sulfonic acid method (TNBS), o-phthalaldehyde method (OPA), hydrated ninhydrin method, and formol titration method. Among them, pH-stat method is used to determine DH using the protons released during titration and hydrolysis process, and it is usually applied only in the hydrolysis of neutral or alkaline environment. OPA, TNBS, and hydrated ninhydrin and formol titration method are all measured by chemical reaction of free amino groups. Among them, the determinations of DH with OPA and TNBS are highly correlated with high accuracy but long time. Hydrated ninhydrin method is generally used for the determination of DH in the low degree of hydrolysis. It is usually possible to select a reasonable DH determination method based on the nature of the hydrolysate, hydrolysis environment, and laboratory conditions.

2.4 Average Peptide Chain Length (PCL)

The PCL of the hydrolysate is usually calculated based on the degree of hydrolysis. If the average chain length of the protein is PCL_0, the formula is established after the protein was hydrolyzed into n peptide molecules:

$$DH = \frac{n-1}{PCL_0 - 1} \times 100\% \tag{9.6}$$

Meanwhile, $PCL_0 = n \times PCL$; the following formula is obtained after putting it into the above equation:

$$DH = \frac{1}{PCL} - \frac{\frac{1}{PCL_0}}{1 - \frac{1}{PCL_0} \times 100\%} \tag{9.7}$$

Because the molecular weight of peanut protein is large, so $\frac{1}{PCL_0} = 0$.

Therefore, $DH = \frac{1}{PCL} \times 100\%$, and thus the following formula is obtained:

$$PCL = \frac{1}{DH} \tag{9.8}$$

3 Preparation Process and Technology

Biological enzyme method was used to hydrolyze the protein under mild conditions, and the generated polypeptide had a very high nutritional value. The modern nutrition study showed (Grimble and Silk 1990; Sheng 1993; Dun and Chen 2004; Zhang and Feng 2004): The oligopeptides with a molecular weight of less than 1000 Da could be easily absorbed by the human body and they had a strong functional activity. This required the selected enzymolysis process to improve the degree of hydrolysis of the protein as far as possible under the premise of ensuring the yield of oligopeptides during the preparation of oligopeptides.

At present, in the process of preparing oligopeptides using proteolysis (Zhang 2002; Guanhong 2005; Mo Qi 1996; Wu and Ding 2002), the enzymolysis time was 360–960 min, the yield of oligopeptides was about 75%, and the degree of hydrolysis of the system was about 16 %. This showed that it was a major problem to be solved how to obtain the oligopeptides with high degree of hydrolysis and yield within a short time. In order to solve the problems of low degree of hydrolysis and yield of peptide products, we prepared peanut oligopeptides using cold-pressed peanut protein powder as the raw material by enzymatic hydrolysis process and strived to prepare the peanut oligopeptides with high yield and degree of hydrolysis through the study on various influencing factors in the enzymatic hydrolysis process and optimization of the process parameters of peanut protein by enzymatic hydrolysis, so as to provide theoretical basis for the industrial production of functional oligopeptides of peanut.

3.1 Enzymolysis Conditions

3.1.1 Single Protease

Enzyme type is one of the most important influencing factors in the enzymatic hydrolysis process. In this experiment, five peanut proteins by protease hydrolysis were selected; the results are shown in Fig. 9.4. Under the recommended operation conditions of various proteases, the TCA-NSI of 1,398 neutral protease, FM, Protamex, N120p-hydrolyzed peanut protein was between 45 and 53% and DH was between 9.4 and 12.1%, while the TCA-NSI and DH of Alcalase-hydrolyzed peanut protein was $63.80 \pm 0.47\%$ and $15.01 \pm 0.88\%$, respectively, which were significantly higher than other proteases ($p < 0.01$). Therefore, Alcalase was selected as the tool enzyme of hydrolyzed peanut protein for the following experiment.

3.1.2 Single-Factor Test of Alcalase-Hydrolyzed Peanut Protein

3.1.2.1 Dosage of Enzyme

In the experiment, the dosage was further improved on the basis of 304 U/g (dosage of enzyme), to study the impact of the dosage of enzyme on TCA-NSI and DH (Fig. 9.5). The results showed that within the concentration range of 304–2428 U/g, the TCA-NSI and DH of enzymatic hydrolysate increased rapidly with the increase of dosage of enzyme. When the dosage of enzyme reached 3642 U/g, the TCA-NSI and DH reached $71.63 \pm 0.16\%$ and $19.74 \pm 0.27\%$, respectively, with an increase of 10.86% and 11.45%, respectively, compared with that when the dosage of enzyme was 304 U/g. When the dosage of enzyme was within the range of 3642–6070 U/g concentration, TCA-NSI basically no longer changed, DH increase was also not obvious, only being 0.85%. In the early stage of enzymatic hydrolysis, macromolecule proteins rapidly decreased, and small-molecule peptide rapidly increased; meanwhile, peptide was further hydrolyzed to the peptide molecules with lower molecular weight as the substrate of protease, and both of them had competitive combination with protease during the hydrolysis process. The initial rate of system reaction would increase with the increase of dosage of enzyme, which made most of large molecular proteins degraded into small-molecule peptides within a short time; when large molecular proteins decreased to a certain extent, regardless of the concentration of protease of the system, the interaction probability between it and large molecular proteins would greatly decreased, and at this time, the main substrate of protease was peptide. Therefore, when the dosage of enzyme reached 3642 U/g, the further increase of dosage of enzyme did not have significant impact on improving the yield of peptide. Although the protease would still have an impact on peptide, DH of the system rose very slowly, because the action sites of protease had been greatly reduced. Thus, when the dosage of enzyme

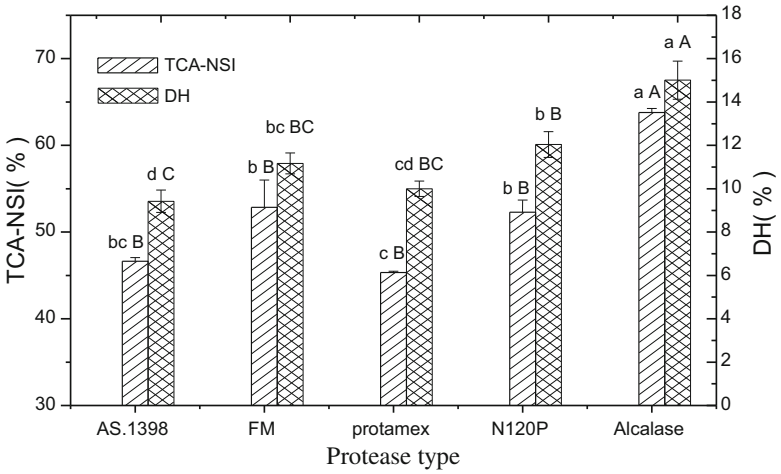

Fig. 9.4 Comparison of effects of enzymatic effects of different proteases (*Note*: Lowercase letters mean 0.05 significance level; capital letters mean 0.01 significance level)

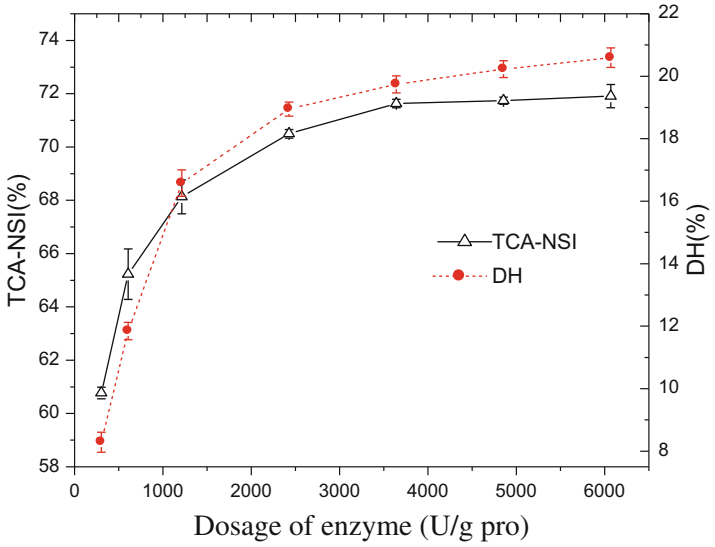

Fig. 9.5 Impact of Alcalase dosage on TCA-NSI and DH

reached 3642 U/g, the yield of oligopeptides of the system is basically unchanged, and the increase range of DH was very small with the further increase of dosage of enzyme, so the appropriate dosage of enzyme was about 3642 U/g.

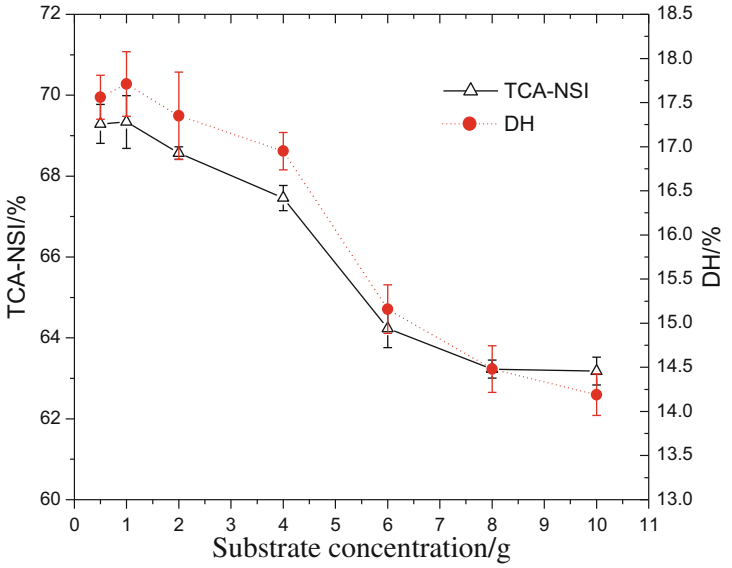

Fig. 9.6 Impact of substrate concentration on TCA-NSI and DH

3.1.2.2 Substrate Concentration

It was shown from Fig. 9.6 that when the substrate concentration was within the range of 1–10%, there was a substrate inhibition in peanut protein-Alcalase system, that is, TCA-NSI and DH decreased with the increase of substrate concentration; the substrate inhibition disappeared when substrate concentration further decreased to 0.5%, and TCA-NSI and DH all decreased compared with substrate concentration of 1%. When the substrate concentration was 4%, TCA-NSI and DH were, respectively, $67.46 \pm 0.31\%$ and $16.95 \pm 0.21\%$, which were lower than that when the substrate concentration was 2% by 1.11% and 0.4%, respectively, and higher than that when the substrate concentration was 6% by 3.23% and 1.79%. It was shown that when the substrate concentration increased from 4% to 6%, the decrease ranges of TCA-NSI and DH were large. In theory, if the system substrate concentration was too large, the effective water concentration would be too low (Tello 1994), thus reducing the diffusion and movement of substrate and protease and inhibiting the hydrolysis; when the substrate concentration was too low, the collision probability of protease and active substrate would be reduced, thus inhibiting the hydrolysis reaction. The experiment results showed that when the substrate concentration was 0.5%, the collision probability of protease and substrate was reduced, the impact of which was larger than that of high effective moisture concentration and reflected in the inhibition of low substrate concentration to hydrolysis; within the concentration range of 1–10%, it was shown by the inhibition of high substrate concentration to hydrolysis reaction, that is, when the substrate concentration was 1%, TCA-NSI and DH reached the maximum values. However,

during the actual production, too low protein concentration in raw materials would result in low absolute yield of product (Deng 1981). Under a condition of a certain amount of processing, it was necessary to increase the output of products by repeated production, which would increase the energy consumption in the production process and reduce equipment utilization, so too low substrate concentration should not be used in the actual production. The substrate concentration of 4% was selected as the optimum substrate concentration in the final experiment.

3.1.2.3 pH Value

The impact of pH on the enzymatic reaction was mainly reflected in the impact on the enzyme activity (Munilla-moran and Saborido-rey 1996). The changes of TCA-NSI and DH when the pH was within the range of 6–9 were analyzed. The results are shown in Fig. 9.7. With the increase of pH value, TCA-NSI and DH rapidly increased; when the system pH reached 8.0, TCA-NSI and DH reached $8.61 \pm 1.23\%$ and $16.36 \pm 0.33\%$, respectively; when the system pH reached 9.0, TCA-NSI and DH decreased compared with that when the pH was 8.0, with a decrease range of 1.59% and 0.84%, respectively. It was shown that Alcalase was more suitable for alkaline environment, so pH 8.0–8.5 was selected as the optimum pH for Alcalase.

3.1.2.4 Reaction Temperature

The changes of TCA-NSI and DH within the temperature range from 40 to 75 °C were analyzed. The results showed that system TCA-NSI and DH increased gradually when the temperature rose from 40 to 55 °C, and system TCA-NSI and DH reached the maximum values at 55 °C, which was $67.70 \pm 0.58\%$ and $15.96 \pm 0.22\%$, respectively. After the temperature exceeded 55 °C, system TCA-NSI and DH began to decrease and then began to decrease rapidly after the temperature exceeded 60 °C. The hydrolysis temperature was closely related to the stability of protease molecules (Wang and Ng 2001), because the peptide bond of protease molecule had a specific spatial structure. If the reaction temperature exceeded a certain limit, the dissociation secondary bond might be caused easily, and thus protein would lose catalytic activity fully or partially. However, if the reaction temperature was too low, the degree of molecular movement of the system would be greatly reduced, and thus the collision probability of protease and substrate would be reduced. Therefore, the action temperature suitable for Alcalase was about 55 °C (Fig. 9.8).

3.1.2.5 Hydrolysis Time

The changes of system TCA-NSI and DH under the impact of different hydrolysis times within the range of 0–240 min were analyzed in this experiment. It was shown

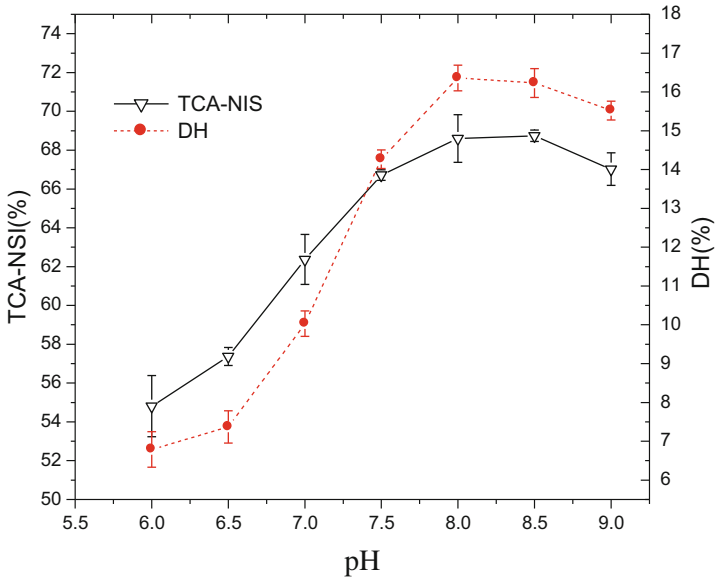

Fig. 9.7 Impact of pH on TCA-NSI and DH

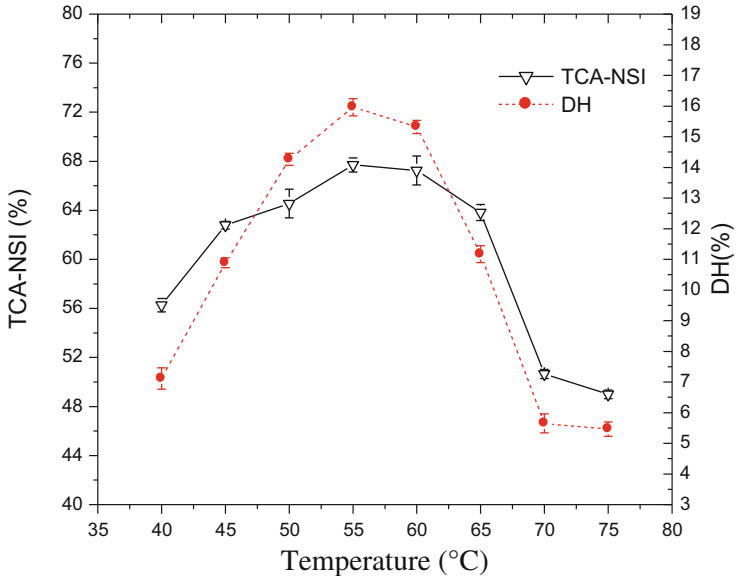

Fig. 9.8 Impact of reaction temperature on TCA-NSI and DH

from Fig. 9.9 that 120 min before hydrolysis, TCA-NSI and DH increased; after hydrolysis for 120 min, TCA-NSI and DH reached $69.69 \pm 0.47\%$ and $15.81 \pm 0.26\%$, respectively; after hydrolysis for 180 min, although DH continued

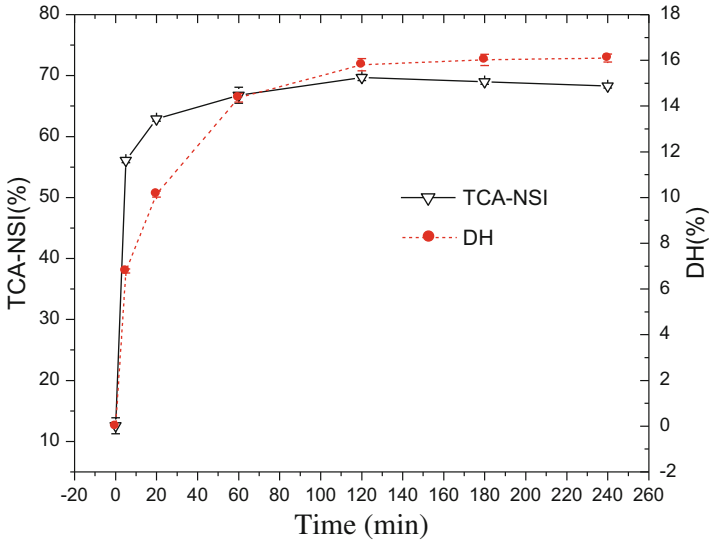

Fig. 9.9 Impact of hydrolysis time on TCA-NSI and DH

to rise, the increase range was only 0.21%, while TCA-NSI showed a decrease trend. This may be due to the fact that Alcalase itself is a complex protease consisting of endonucleases and enzymes. During the hydrolysis process, the activity of enzyme might gradually appear with the gradual decrease of endonuclease sites, and some peptide molecules of the system were hydrolyzed to amino acids under the action of enzyme in the hydrolysis system. In the later stage of hydrolysis, the hydrolysis rate of endonucleases of the system was greater than that of enzyme. Therefore, after 180 min, the peptide extraction rate of the system slightly decreased. It was shown that when the hydrolysis time was 120 min, the extraction rate of peptide of the system reached the maximum value. At this time, the increase range of the degree of hydrolysis was very small with the extension of hydrolysis time. Therefore, it was determined that the optimum hydrolysis time was about 120 min.

3.1.3 Orthogonal Rotation Combination Experiment of Alcalation Hydrolyzed Peanut Protein

The results of TCA-NSI and DH measured through 23 treatment combination experiments of four-factor quadratic rotation combination are shown in Table 9.5. SPSS working platform was used to analyze and process the results, establish the mathematical models of TCA-NSI and DH with various factors, obtain the optimum process conditions by taking TCA-NSI as the first indicator and using the analysis of oligopeptide yield model, and determine the degree of hydrolysis of the system using DH model under the optimal conditions.

Table 9.5 Results of orthogonal rotation experiment

Processing number	Matrix design				TCA-NSI/%			Degree of hydrolysis/%		
	X1	X2	X3	X4	Experiment value	Fitted value	Fitted error	Experiment value	Fitted value	Fitted error
1	1	1	1	1	62.79	61.37	1.42	11.39	12.04	−0.65
2	1	1	−1	−1	48.80	49.68	−0.88	5.16	4.98	0.18
3	1	−1	1	−1	65.45	62.54	2.91	10.02	9.54	0.48
4	1	−1	−1	1	58.80	58.07	0.73	10.53	11.36	−0.83
5	−1	1	1	−1	71.97	70.57	1.40	11.61	11.62	−0.01
6	−1	1	−1	1	66.57	66.10	0.47	13.81	13.44	0.37
7	−1	−1	1	1	75.65	78.96	−3.31	17.21	18.00	−0.79
8	−1	−1	−1	−1	65.90	67.27	−1.37	10.01	10.94	−0.93
9	−1.682	0	0	0	72.20	70.36	1.84	12.59	12.39	0.20
10	1.682	0	0	0	46.50	48.82	−2.32	5.49	5.63	−0.14
11	0	−1.682	0	0	80.21	79.27	0.94	15.52	14.89	0.63
12	0	1.682	0	0	70.13	71.24	−1.11	11.06	11.63	−0.57
13	0	0	−1.682	0	64.56	63.77	0.79	12.17	12.81	−0.64
14	0	0	1.682	0	76.08	77.35	−1.27	16.43	17.21	−0.78
15	0	0	0	−1.682	60.60	61.65	−1.05	8.59	9.07	−0.48
16	0	0	0	1.682	68.29	67.72	0.57	17.05	16.54	0.51
17	0	0	0	0	75.16	75.26	−0.10	16.14	15.01	1.13
18	0	0	0	0	74.47	75.26	−0.79	14.52	15.01	−0.49
19	0	0	0	0	76.08	75.26	0.82	15.76	15.01	0.75
20	0	0	0	0	73.56	75.26	−1.70	13.91	15.01	−1.10
21	0	0	0	0	78.15	75.26	2.89	14.52	15.01	−0.49
22	0	0	0	0	74.47	75.26	−0.79	15.29	15.01	0.28
23	0	0	0	0	75.16	75.26	−0.10	14.91	15.01	−0.10

3.1.3.1 Impact of Enzymatic Hydrolysis on TCA-NSI

SPSS data processing system was used to fit the experimental data by standard polynomial regression method, thus establishing the quadratic polynomial Formula 9.9:

$$\begin{aligned} Y = \; & 75.22 - 6.40X1 - 2.39X2 + 4.04X3 + 1.80X4 \\ & -5.54X12 + 0.06X22 - 1.66X32 - 3.74X42 \\ & -0.60X1X2 + 0.34X1X3 + 0.19X1X4 + 0.19X2X3 \\ & +0.34X2X4 - 0.60X3X4 \end{aligned} \tag{9.9}$$

After excluding the nonsignificant items at $\alpha = 0.05$ significance level, the simplified regression equation is Formula 9.10:

$$Y = 75.22 - 6.4X1 - 2.39X2 + 4.04X3 + 1.8X4 - 5.54X12 - 1.66X32 - 3.74X42 \tag{9.10}$$

To test the significance of regression equation, F-test should be conducted to the regression equation. The results are shown in Table 9.6. From $F_{0.05}\,(2, 6) = 5.14 < F_1 = 5.641 < F_{0.01}\,(2, 6) = 10.92$. It was shown that the item in lack of fit was significant at the level of $\alpha = 0.05$, but it was nonsignificant at the level of $\alpha = 0.01$, indicating that there were factors in lack of fit and this might come from the high-order interaction between the factors. From $F_2 = 25.106 > F_{0.01}\,(9, 15) = 5.56$, it was shown that the regression equation itself was significant at the level of $\alpha = 0.01$, and the maximum fitting error between fitting value and experiment value was 5.0%, indicating that the regression equation and the experiment were fitted properly.

After the model was established, further analysis was made to the characteristics of the model, and the regression equation model (9.9) was rewritten as a matrix (Eq. 9.1) form:

$$[y] = 107.42 + \begin{bmatrix} x_1 \\ x_2 \\ x_3 \\ x_4 \end{bmatrix}^T \begin{bmatrix} -6.40 \\ -2.39 \\ 4.04 \\ 1.80 \end{bmatrix} + \begin{bmatrix} x_1 \\ x_2 \\ x_3 \\ x_4 \end{bmatrix}^T A \begin{bmatrix} x_1 \\ x_2 \\ x_3 \\ x_4 \end{bmatrix} \tag{9.11}$$

where

$$A = \begin{bmatrix} -11.08 & -0.60 & 0.34 & 0.19 \\ -0.60 & 0.12 & 0.19 & 0.34 \\ 0.34 & 0.19 & -3.32 & -0.60 \\ 0.19 & 0.34 & -0.60 & -7.48 \end{bmatrix}$$

To obtain the stationary points of Formula 9.11, set:

Table 9.6 Variance analysis of TCA-NSI test results

Source of variation	Quadratic sum	Degree of freedom	Mean square	Ratio F	Significance level p
X_1	560.2580	1	560.2580	118.10791	0.00000
X_2	77.9261	1	77.9261	16.42759	0.00367
X_3	222.8255	1	222.8255	46.97381	0.00013
X_4	44.3946	1	44.3946	9.35883	0.01560
X_1^2	480.9496	1	480.9496	101.38891	0.00001
X_2^2	0.2693	1	0.2693	0.05678	0.81766
X_3^2	40.4939	1	40.4939	8.53650	0.01924
X_4^2	216.1033	1	216.1033	45.55671	0.00015
X_1X_2	5.8182	1	5.8182	1.22653	0.30027
X_1X_3	1.8831	1	1.8831	0.39698	0.54622
X_1X_4	0.5586	1	0.5586	0.11775	0.74033
X_2X_3	0.5586	1	0.5586	0.11775	0.74033
X_2X_4	1.8831	1	1.8831	0.39698	0.54622
X_3X_4	5.8182	1	5.8182	1.22653	0.30027
Regression	1667.2850	14	119.0918	$F_2 = 25.106$	
Residue	37.9489	8	4.7436		
Lack of fit	24.7737	2	12.3869	$F_1 = 5.641$	
Error	13.1751	6	2.1959		
Sum	1705.2241	22			

$$\frac{\partial y}{\partial x} = \left(\frac{\partial y}{\partial x_1} \cdots \frac{\partial y}{\partial x_4}\right)^T = 0 \tag{9.12}$$

The stationary points can be obtained from Formula 9.12: $x_1 = -0.578$, $x_2 = -1.682$, $x_3 = 1.197$, and $x_4 = 0.241$.

Judge whether the stationary points were saddle points, and determine the properties of positive and negative of Matrix A, and establish Formula 9.13:

$$|A - \lambda I| = 0 \tag{9.13}$$

After solving the opposite sign of λ value, it was shown that Matrix A was negative, so this stationary point was saddle point, and y only had the maximum value.

From this, the optimal combination when TCA-NSI was the maximum included: hydrolysis temperature, 53 °C; substrate concentration, 1%; dosage of enzyme, 3637 U/g; and hydrolysis time, 105 min, which were basically consistent with single-factor test results. Under this condition, the yield of oligopeptide measured in the test under this condition was 83.8%.

From the results of the model analysis, it was found that the enzymatic hydrolysis efficiency decreased gradually with the increase of the protein concentration

within the selected range. However, the increase of the protein concentration in the production could reduce the energy consumption and improve the utilization rate of the equipment. Therefore, a high substrate concentration could be selected according to the model during the actual production. The single-factor test showed that 4% was the optimum substrate concentration, so 4% was chosen as the optimum substrate concentration. Combined with the regression model, it was found that the TCA-NSI of the system was 80.35% when the substrate concentration was 4% and other factors were under the best conditions.

3.1.3.2 Impact of Enzyme Hydrolysis on DH

SPSS data processing system was used to fit the test data by standard polynomial regression method, thus establishing the quadratic polynomial formula 9.14:

$$\begin{aligned} Y = \; & 15.01 - 2.01X1 - 0.97X2 + 1.31X3 + 2.22X4 \\ & -2.12X12 - 0.62X22 - 0.26X32 - 0.78X42 \\ & -0.14X1X2 + 0.05X1X3 + 0.17X1X4 + 0.17X2X3 \\ & +0.05X2X4 - 0.14X3X4 \end{aligned} \tag{9.14}$$

After excluding the nonsignificant items at $\alpha = 0.05$ significance level, the simplified regression equation is Formula 9.15:

$$\begin{aligned} Y = {} & 15.01 - 2.01X1 - 0.97X2 + 1.31X3 + 2.22X4 - 2.12X12 \\ & - 0.62X22 - 0.78X42 \end{aligned} \tag{9.15}$$

To test the significance of regression equation, F-test should be conducted to the regression equation. The results are shown in Table 9.7. From $F_1 = 8.785 < F_{0.05}(2, 6) = 5.14$, it was shown that the item in lack of fit was not significant at the level of $\alpha = 0.05$, indicating that there were no factors in lack of fit. From $F_2 = 24.64 > F_{0.01}\ (9, 15) = 5.56$, it was shown that the regression equation itself was significant at the level of $\alpha = 0.01$ and the maximum fitting error between fitting value and experiment value was 9.29%, indicating that the regression equation and the experiment were fitted properly.

After substituting the optimal combination, namely, $x_1 = -0.578$, $x_2 = -0.238$, $x_3 = 1.197$, and $x_4 = 0.241$, into DH regression model, it was found that the system DH acting under this condition was DH = 17.72 %, PCL = 5.64, and Mw = 638.4.

3.1.4 Screening of Compound Enzymatic Proteases

Enzyme type is one of the most important factors in the enzymatic process. In this test, Alcalase was used to hydrolyze peanut protein, and then four kinds of proteases were used to continue enzymolysis for peanut protein respectively. The results are shown in Fig. 9.10. Under the recommended conditions of various proteases, the

Table 9.7 Variance analysis of DH test results

Source of variation	Quadratic sum	Degree of freedom	Mean square	Ratio F	Significance level p
X_1	55.2975	1	55.2975	76.88987	0.00002
X_2	12.9540	1	12.9540	18.01224	0.00282
X_3	23.4207	1	23.4207	32.56591	0.00045
X_4	67.5275	1	67.5275	93.89534	0.00001
X_1^2	70.6569	1	70.6569	98.24665	0.00001
X_2^2	5.6395	1	5.6395	7.84157	0.02319
X_3^2	0.8864	1	0.8864	1.23257	0.29916
X_4^2	9.2521	1	9.2521	12.86475	0.00712
X_1X_2	0.3025	1	0.3025	0.42062	0.53480
X_1X_3	0.0324	1	0.0324	0.04505	0.83722
X_1X_4	0.4422	1	0.4422	0.61490	0.45554
X_2X_3	0.4422	1	0.4422	0.61490	0.45554
X_2X_4	0.0324	1	0.0324	0.04505	0.83722
X_3X_4	0.3025	1	0.3025	0.42062	0.53480
Regression	248.1178	14	17.7227	$F_2 = 24.643$	
Residue	5.7534	8	0.7192		
Lack of fit	2.1355	2	1.0677	$F_1 = 1.771$	
Error	3.6179	6	0.6030		
Sum	253.8704	22			

DH of peanut proteins which were Alcalase hydrolyzed by N120P and FM were significantly higher than that of other two proteases, being $20.96 \pm 0.33\%$ and $20.08 \pm 0.37\%$, respectively, and there were no significant difference between them ($p > 0.05$); the TCA-NSI value of peanut protein Alcalase hydrolyzed by N120P reached $84.6 \pm 0.74\%$, which increased by 6.45% compared with that hydrolyzed by Alcalase alone and was significantly higher than that of other protease ($P < 0.05$). It was shown that in the enzymatic hydrolysate of peanut protein Alcalase hydrolyzed by N120P, DH and the yield of oligopeptide were all high; therefore, N120P was selected as the tool enzyme for Alcalase hydrolyze peanut protein in the following study.

3.1.5 Single-Factor Test of N120P-Hydrolyzed Peanut Protein

3.1.5.1 Dosage of Enzyme

The test analyzed the changes of the system TCA-NSI and DH when the N120P concentration was within the range of 300–3600 U/g (Fig. 9.11). The results showed that with the increase of the dosage of N120P, the TCA-NSI and DH in enzymatic hydrolysate gradually rose. When the dosage of N120P was smaller than 1800 U/g, the increase speeds of TCA-NSI and DH were quick; when the dosage of

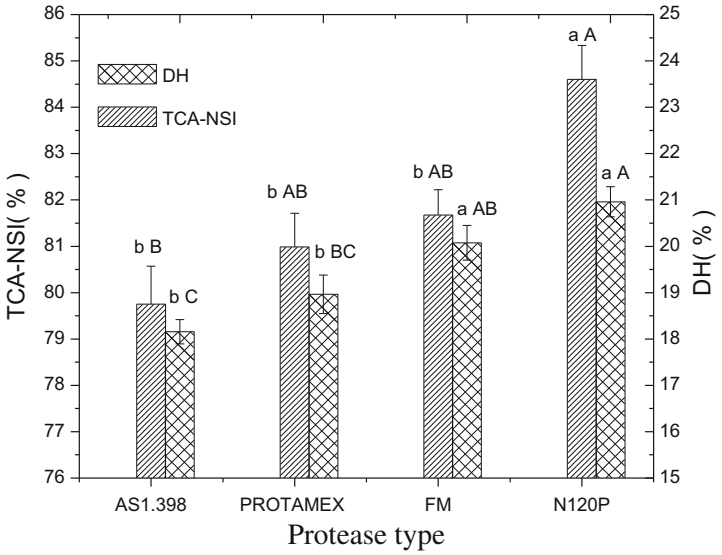

Fig. 9.10 Screening of compound enzymolysis protease

N120P reached 1800 U/g, TCA-NSI and DH were $54.44 \pm 0.42\%$ and $13.89 \pm 0.44\%$, respectively; and when the dosage of enzyme was within the range of 1800–3600 U/g, the increase ranges of TCA-NSI and DH were only 1.17% and 0.707%. According to enzyme kinetics, too large or too small dosage of enzyme was unfavorable to hydrolysis, and too large dosage of enzyme could not achieve the hydrolysis effect but might cause the waste of resources. So the appropriate dosage of enzyme should be 1800 U/g.

3.1.5.2 pH Value

The impact of pH value on enzymatic reaction was mainly reflected in enzyme activity. The test analyzed the changes of the system TCA-NSI and DH when pH value was within the range of 5–8. It was shown in Fig. 9.12 that TCA-NSI and DH gradually increased with the increase of pH value and TCA-NSI and DH reached the maximum values when pH value was 6.0, being $51.94 \pm 0.42\%$ and $13.83 \pm 0.34\%$, respectively; when the pH value was greater than 6.0, TCA-NSI and DH began to decrease. This showed that too acidic or alkaline system would affect the activity of enzyme; N120P was more suitable for neutral to acidic conditions, so pH 6.0 was selected as the optimal pH.

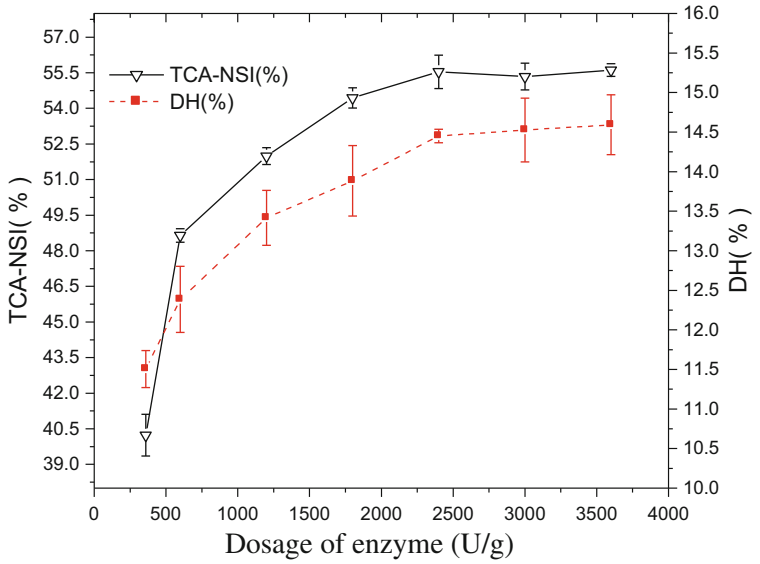

Fig. 9.11 Impact of dosage of N120P on TCA-NSI and DH

3.1.5.3 Reaction Temperature

The activity of the enzyme depends largely on the temperature used. This test analyzed the changes in TCA-NSI and DH over the temperature range from 40 to 70 °C. As shown in Fig. 9.13, the system TCA-NSI and DH increased greatly when the temperature rose from 40 to 55 °C, and system TCA-NSI and DH reached the maximum values at 55–60 °C, being 53.29 + 1.48 % and 13.97 + 0.56 %, respectively; system TCA-NSI and DH began to decrease after the temperature reached 60 °C. This was because the peptide bond of protease molecule had a specific spatial structure. If the reaction temperature exceeded a certain limit, the molecule would absorb too much energy and thus cause the secondary bonds to disintegrate or lose fully or partially its catalytic activity (Wang and Gu 1999). Therefore, the temperature suitable for N120P might be between 5 and 60 °C.

3.1.5.4 Reaction Time

This test analyzed the impacts of different enzymolysis times within the range of 0–240 min on system TCA-NSI and DH. It was shown from Fig. 9.14 that 20 min before enzymolysis, TCA-NSI and DH increased rapidly; however, after 20 min, the increase speed began to slow down; TCA-NSI and DH reached 48.99 ± 1.34 % and 12.8 ± 0.37%, respectively, at 60 min. However, when the enzymolysis time was within the range of 60–240 min, the increase ranges of TCA-NSI and DH were

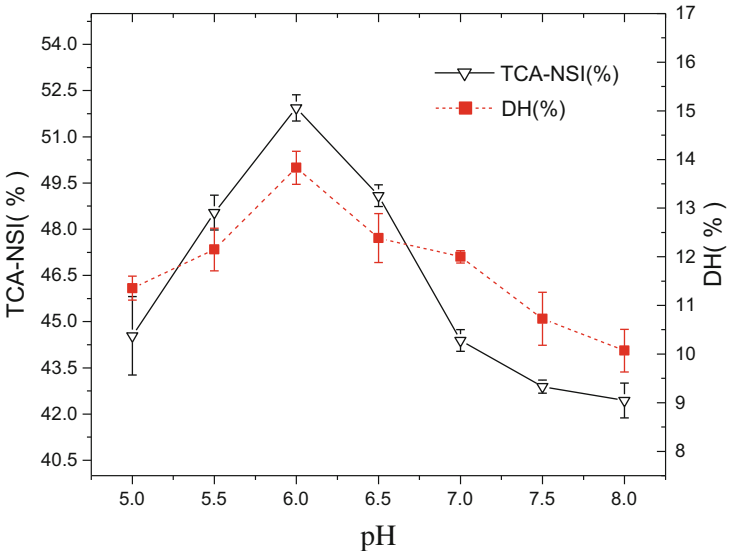

Fig. 9.12 Impact of pH on TCA-NSI and DH

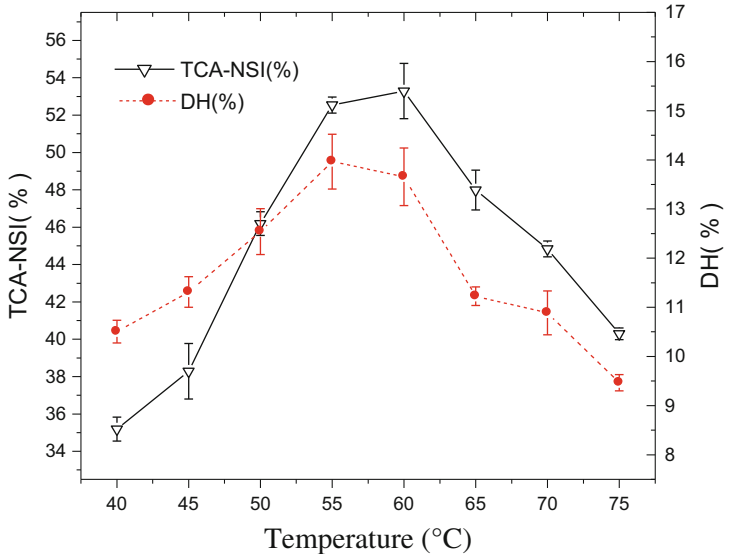

Fig. 9.13 Impact of temperature on TCA-NSI and DH

only 2.92% and 1.21%. The increase speed was very slow, so the suitable time was about 60 min.

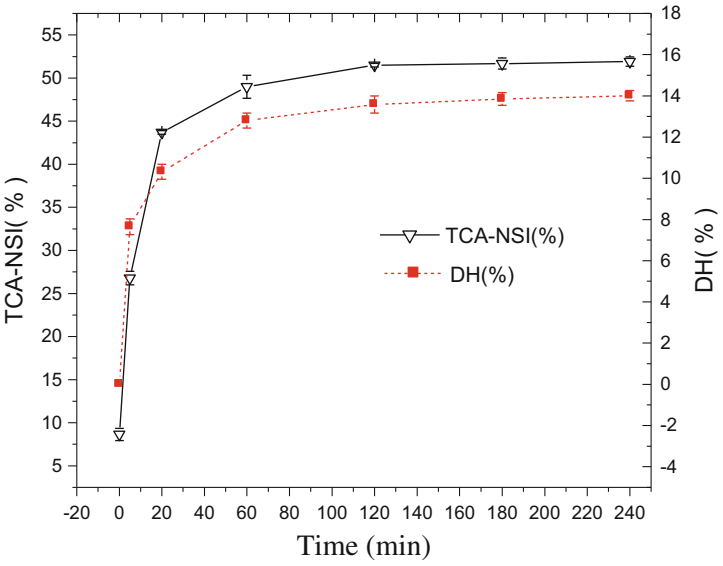

Fig. 9.14 Impact of time on TCA-NSI and DH

3.1.5.5 Uniform Design of N120P-Hydrolyzed Peanut Protein

The results of the TCA-NSI measured by 11 treatment combinations with uniform design are shown in Table 9.8. SPSS working platform was used to analyze and process the results and establish the mathematical model for the relationship between TCA-NSI and various factors, and the optimum process conditions were obtained by analyzing the model.

Quadratic polynomial stepwise regression analysis was conducted to the test results. Take the multiple correlation coefficient R as the indicator and semiautomatically delete the nonsignificant items in the equation, thus establishing the following regression model finally:

$$Y = 67.852 + 2.450X2 + 4.480X3 - 0.057X12 - 0.143X22 - 0.273X32 + 0.045X1X3 - 0.172X2X3$$

The correlation coefficients of regression model: $R^2 = 0.98269$, $P = 0.0328$, equation Durbin-Watson statistics $d = 1.76122687$, indicating that the residuals are independent of each other. The maximum fitting error between fitted value and test value was 2.77%, indicating that the fitting between regression equation and test was good, and the regression model established in this test was credible.

The intuitive judgment based on the three-dimensional response diagram of all factors is shown in Fig. 9.15. The optimal combination when the regression model TCA-NSI was highest was $X_1 = 2.81124$, $X_2 = 4.31006$, and $X_3 = 7.08699$, that is, hydrolysis time was 65 min, hydrolysis temperature was 57 °C, and the enzyme-

Table 9.8 Results of uniform design test

Processing number	Time (min)	Temperature (°C)	Dosage of enzyme (U/g)	TCA-NSI(%)		
				Actual value	Fitted value	Fitting error
1	5	6	11	84.00	83.27	0.73
2	7	1	4	81.23	84.21	−2.98
3	10	9	2	77.79	78.39	−0.60
4	9	3	10	85.40	85.13	0.27
5	6	11	5	83.77	82.69	1.08
6	4	4	1	78.47	78.54	−0.07
7	8	8	8	84.00	83.66	0.34
8	3	10	9	81.23	83.48	−2.25
9	2	2	7	88.21	88.32	−0.12
10	1	7	3	85.17	83.10	2.07
11	11	5	6	85.40	83.87	1.53

substrate ratio was 2061 U/g, which was basically consistent with that of single-factor test results. The TCA-NSI measured under this condition was 89.01%, which was 10.86% higher than that under the single action of Alcalase.

3.1.5.6 Determination of DH of Peanut Protein Compound Enzymatic Hydrolysate

The compound enzymolysis time of peanut protein under the optimal conditions was 170 min; the degree of hydrolysis DH of the system was $23.76 \pm 0.93\%$, which was 6.24% higher than that of single enzymolysis by Alcalase; PCL was 4.21 ± 0.16, which was1.5 lower than that of single enzymolysis by Alcalase; and the average molecular weight of the system was 481.1. It was shown that compound enzymolysis could greatly increased the yield of peanut functional oligopeptides and significantly decreased the length of peptides in peanut functional oligopeptide system ($p < 0.01$).

3.2 Enzymolysis Kinetics

The enzymatic preparation of oligopeptides refers to optimizing the hydrolysis parameters, determining the relationship between the degree of hydrolysis of the products and molecular weight distribution, and thus obtaining the oligopeptides with the target molecular weight distribution through the study on protein enzymolysis conditions, degree of hydrolysis and the molecular weight distribution

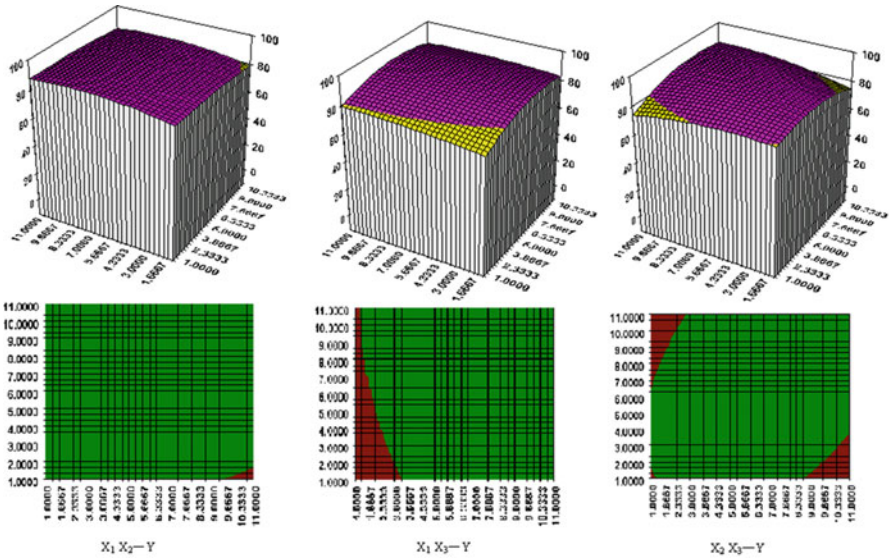

Fig. 9.15 Response surface diagram of interaction of factors on compound enzymolysis

of hydrolysis products, and other indicators. The enzymolysis of protein is a complex process. Protein may contain different types of peptide bonds, and proteases may have different degrees of hydrolysis on different peptide bonds. Due to this, sometimes it may be difficult to clearly describe and explain the protein hydrolysis process. Therefore, it is of practical significance for the deep understanding of the protein hydrolysis process to derive the kinetic relationship formula for describing the enzymatic hydrolysis process law of protein, calculate the kinetics parameters of the enzyme, and establish the experimental model that is consistent with the experimental data from the reaction mechanism.

A large amount of data, derivation, operation, and repeated verification were required to establish the polymer substrate hydrolysis kinetics model that could reflect the hydrolysis process, and the whole process needs to take a lot of time; the model established only relying on the fitting of several sets of data could not reflect the entire hydrolysis process. In response to this problem, Marquez and Fernandez (1993) argued that for the hydrolysis reaction with the same mechanism, the model established before could be used to combine with the actual data for constructing the kinetic curve of hydrolysis process and thus obtaining some information in the hydrolysis process.

3.2.1 Kinetic Model of Enzymolysis

3.2.1.1 Kinetic Model of Single Enzymolysis

The enzymatic hydrolysis reaction of protein should meet the double-substrate sequence reaction mechanism, and it was composed of the following steps. In the aqueous solution, the second step was to limit the speed, and the reverse process was negligible:

$$E + S \underset{K-1}{\overset{K_1}{\rightleftarrows}} ES \tag{9.16}$$

$$ES + \mathrm{H_2O} \overset{K_2}{\rightarrow} E + P - \mathrm{OH} + H - P \tag{9.17}$$

$$ES + S \underset{K-3}{\overset{K_3}{\rightleftarrows}} ES_2 \tag{9.18}$$

Therefore, the derivative equation with the following reaction rate could be reached. The reaction rate was represented by R, and S_0 represented the initial substrate concentration:

$$R = S_0 \frac{\mathrm{d}(DH)}{\mathrm{d}(t)} = K_2|ES| \tag{9.19}$$

In the enzymatic reaction process, the reaction formula of the protease being passivated due to the inhibition of substrates and products was as follows, where E_a represented the active protease and E_i represented the passivated protease:

$$E + ES \overset{K_d}{\rightarrow} E_a + E_i + S \tag{9.20}$$

The kinetic equation of the above reaction process was

$$-\frac{\mathrm{d}e}{\mathrm{d}t} = K_d|E||ES| \tag{9.21}$$

The following formula was established after dividing Eq. 9.19 by Eq. 9.21:

$$-S_0 \frac{\mathrm{d(DH)}}{\mathrm{d}e} = \frac{K_2}{K_d|E|} \tag{9.22}$$

There were two existence forms of protease in the hydrolysis system: one was free state E, the other was complex state ES, and total protease should be the sum of these two parts. Therefore:

$$e = |E| + |ES| \tag{9.23}$$

When in the equilibrium and stabilization phase, the produced ES complex was equal to the decomposed ES complex, thus establishing the following equation:

$$K_1|E||S| = (K_1 + K_2)|ES| \tag{9.24}$$

$$|ES| = \frac{K_1|E||S|}{K_1 + K_2} = \frac{|E||S|}{K_m} \tag{9.25}$$

$$K_m = \frac{K_1 + K_2}{K_1} \tag{9.26}$$

After substituting Eq. 9.25 into Eq. 9.23, and setting $|S| = S_0$, the following equation was established:

$$|E| = \frac{K_m e}{K_m + S_0} \tag{9.27}$$

K_m was Michaelis-Menten constant, and its physical meaning was the substrate concentration in mol/L when the enzyme reaction rate reached half the maximum reaction rate. K_m could only be used to determine the specificity of enzyme and natural substrate, $\frac{1}{Km}$ could approximately represent the size of the enzyme affinity for the substrate, and the greater the $\frac{1}{K_m}$ was, the larger the affinity was because the greater the $\frac{1}{K_m}$ was, the smaller the substrate concentration required to achieve half of the maximum reaction rate was. Obviously, when r optimal substrate was reached, the enzyme affinity was the largest, while K_m was the smallest. The K_m values of enzyme preparations measured at present were all small, so $K_m << S_0$ was set, and Eq. 9.27 could be simplified as:

$$|E| = \frac{K_m e}{S_0} \tag{9.28}$$

After substituting Eq. 9.28 into Eq. 9.22, the following equation was established:

$$-\frac{\mathrm{d(DH)}}{\mathrm{d}e} = \frac{K_2}{K_d K_m} * \frac{1}{e} \tag{9.29}$$

After definite integration for Eq. 9.29, the upper and lower limits of the degree of hydrolysis were DH and 0, respectively, while the upper limit of total enzyme amount e was e, its lower limit was e_0; therefore, its integral equation was:

$$\int_{e0}^{e} \frac{\mathrm{d}e}{e} = -\frac{K_d K_m}{K_2} \int_0^{\mathrm{DH}} \mathrm{d(DH)} \tag{9.30}$$

The following equation was established by integration of the both sides of Eq. 9.30:

$$\ln e - \ln e_0 = -\frac{K_d K_m}{k_2}(\mathrm{DH}) \tag{9.31}$$

After simplifying the equation, the following formula was established:

$$e = e_0\left[-\frac{K_d K_m}{K_2}(\mathrm{DH})\right] \tag{9.32}$$

Through arranging Eqs. 9.19, 9.25, 9.28, and 9.32, the following formula was established:

$$R = K_2 e_0 \exp\left[-\frac{K_d K_m}{K_2}(\mathrm{DH})\right] \tag{9.33}$$

After merging Eq. 9.19 with Eq. 9.33, the following formula was established:

$$\frac{\mathrm{d}(\mathrm{DH})}{\mathrm{d}t} = \frac{K_2 e_0}{S_0}\exp\left[-\frac{K_d K_m}{K_2}(\mathrm{DH})\right] \tag{9.34}$$

Based on the previous study results, the kinetic model of the single enzyme hydrolysis process of protein was:

$$\frac{\mathrm{d}(\mathrm{DH})}{\mathrm{d}t} = a\exp[-b*(\mathrm{DH})] \tag{9.35}$$

From Eqs. 9.34 and 9.35, the following equations were established:

$$a = \frac{K_2 e_0}{S_0} \tag{9.36}$$

$$b = \frac{K_d K_m}{K_2} \tag{9.37}$$

Therefore, the kinetic model of single enzyme hydrolysis process of protein was based on Eqs. 9.33, 9.36, and 9.37:

$$R = aS_0\exp[-b(\mathrm{DH})] \tag{9.38}$$

From Formula 9.36, it was shown that the size of a was related to the initial substrate concentration and the initial protease concentration of the enzymolysis system and it decreased with the increase of the initial substrate concentration and increased with the increase of the initial protease concentration. Because K_2 was related to hydrolysis temperature, the size changed with the change in hydrolysis

temperature. From Formula 9.37, the size of b was not related to the initial protein concentration and the initial protease concentration but related to the hydrolysis temperature. In the constant temperature hydrolysis reaction, the size of b should be a constant; the size of a was only related to the initial substrate concentration of the enzymolysis system and the initial protease concentration. From Eq. 9.38, the larger the value of a was, the greater the reaction rate was; when a was less than 0 and R was negative, enzymatic reaction could not be carried out.

3.2.1.2 Kinetic Model of Compound Enzymolysis

Compound enzymolysis refers to the process that the second enzyme continues to hydrolyze the substrate after the first enzyme. Although the action conditions were different, at this time, the first enzyme in the system still had a weak hydrolysis on the substrate, and it played a certain role in promotion relative to the second enzyme; on the other hand, some sites of the second enzyme had been cut by the first enzyme, so it reduced part of the activity of the second enzyme. Therefore, when making definite integration for Formula 9.29, the lower limit of total enzyme amount e was set to be e_0–c, and thus the following integral equation was established:

$$\int_{e_0-c}^{e} \frac{\mathrm{d}e}{e} = -\frac{K_d K_m}{K_2} \int_0^{\mathrm{DH}} d(\mathrm{DH}) \tag{9.39}$$

The following formula was established after integration of the both sides:

$$\ln e - \ln e_0 - c = -\frac{K_d K_m}{k_2}(\mathrm{DH}) \tag{9.40}$$

After making simplification:

$$e = (e_0 - c)\left[-\frac{K_d K_m}{K_2}(\mathrm{DH})\right] \tag{9.41}$$

By arranging Eqs. 9.19, 9.25, 9.28, and 9.32, the following equation was established:

$$R = K_2(e_0 - c)\exp\left[-\frac{K_d K_m}{K_2}(\mathrm{DH})\right] \tag{9.42}$$

After merging Eq. 9.19 with Eq. 9.42, the following equation was established:

$$\frac{\mathrm{d(DH)}}{\mathrm{d}t} = \frac{K_2(e_0 - c)}{S_0} \exp\left[-\frac{K_d K_m}{K_2}(\mathrm{DH})\right] \tag{9.43}$$

The following equation was established based on Eqs. 9.42 and 9.43:

$$a = \frac{K_2 e_0}{S_0} - \frac{K_2 c}{S_0}\, b = \frac{K_d K_m}{K_2} \tag{9.44}$$

The c value in Eq. 9.44 was produced due to the action of the first enzyme on the substrate, so $c = c_0 S_0$, and the following equation was established:

$$a = \frac{K_2 e_0}{S_0} - K_2 c_0 \tag{9.45}$$

3.2.2 Kinetics Model Parameters

The nonlinear regression model was used to fit the sets of data with different substrate concentrations and different enzyme concentrations, derive the kinetics model parameters during the enzymolysis process, effectively establish the kinetics model of enzymolysis process, and explain the phenomenon of the enzymolysis process based on this. Zhang Yuhao and Wang Qiang (2007) derived the kinetics parameters of the hydrolysis process of main tool enzyme Alcalase and auxiliary tool enzyme N120P during the preparation of peanut oligopeptide and established the corresponding kinetics model. The derivation results and process are as follows.

Nonlinear regression model was used to fit the sets of data with different substrate concentrations and different enzyme concentrations and derive the kinetics model parameters of Alcalase enzymolysis peanut protein based on this. The fitting effect was good when using logarithm model. The details are shown in Table 9.9.

Logarithm model is represented as $y = c - d\ln(x + f)$, and the following formula is established after differentiation:

$$\mathrm{d}x = -\frac{\exp\left(\frac{c-y}{d}\right)}{d}\mathrm{d}y \tag{9.46}$$

$$\text{So} \quad \frac{\mathrm{d}y}{\mathrm{d}x} = -d \times \exp\left(-\frac{c}{d}\right) \times \exp\left(\frac{y}{d}\right) \tag{9.47}$$

In contrast with Eq. 9.35, the following formula is established:

$$a = -d \times \exp\left(-\frac{c}{d}\right) \tag{9.48}$$

Table 9.9 Fitting result of logarithm model to Alcalase

Sample	Equation	Related coefficient
Substrate concentration 4%	$DH = 1.62146 + 2.99959^{*} \ln(t + 0.59445)$	0.9867
Substrate concentration 6%	$DH = 0.09613 + 2.99061^{*} \ln(t + 0.99643)$	0.9874
Substrate concentration 8%	$DH = -0.37737 + 2.97314^{*} \ln(t + 1.17604)$	0.9858
Substrate concentration 10%	$DH = -1.11463 + 2.95763^{*} \ln(t + 1.52124)$	0.9887
Dosage of enzyme 606	$DH = -3.9214 + 2.95251^{*} \ln(t + 3.99737)$	0.9902
Dosage of enzyme 1214	$DH = -0.43601 + 3.00082^{*} \ln(t + 1.20441)$	0.9809
Dosage of enzyme 3642	$DH = 2.84359 + 3.00759^{*} \ln(t + 0.38989)$	0.9983

$$b = -\frac{1}{d} \tag{9.49}$$

The kinetics parameters a and b corresponding to different initial substrate concentrations and initial protease concentrations in the process of Alcalase enzymolysis peanut protein were obtained based on Table 9.9 and Eqs. 9.48 and 9.49, as shown in Table 9.10:

As can be seen from the experimental results in Table 9.10, the kinetics parameter a decreased with the increase of initial substrate concentration and increased with the increase of initial Alcalase concentration. There was a small difference in kinetics parameter b, and it was close to a constant and fluctuated up and down near its average value of 0.3352 under different initial substrate concentrations and initial protease concentrations. Therefore, in a constant temperature hydrolysis reaction, b could be regarded as a constant, which was consistent with the conclusion of the model derivation.

From Eq. 9.36, it was known that the value was the ratio between initial protease concentration and initial substrate concentration during the constant temperature hydrolysis reaction, that is, E_0/S_0 was in a linear relationship. Therefore, relevant data were extracted from Table 9.10 for linear fitting, as shown in Fig. 9.16.

The linear relationship formula $y = 254.65x$, $R^2 = 0.9903$ obtained from Fig. 9.16 was consistent with Eq. 9.36, so the equation corresponding to the relationship curve of a value and E_0/S_0 value was:

$$a = 254.65\frac{E_0}{S_0} \tag{9.50}$$

In contrast with Eqs. 9.36 and 9.50, $K_2 = 254.65$ (min^{-1}) was established.

After substituting a and b values into Eq. 9.38, the kinetics model of Alcalase enzymolysis peanut protein was established:

Table 9.10 Kinetics parameters of Alcalase enzymolysis

S_0 (g/L)	E_0 (g/L)	E_0/S_0 (g/g)	a (min^{-1})	b
100	0.8	0.008	2.0290	0.3381
80	0.8	0.010	2.6187	0.3363
60	0.8	0.013	3.0880	0.3344
40	0.8	0.020	5.1502	0.3334
40	0.2	0.005	0.7823	0.3387
40	0.4	0.010	2.5950	0.3332
40	1.2	0.030	7.7416	0.3325

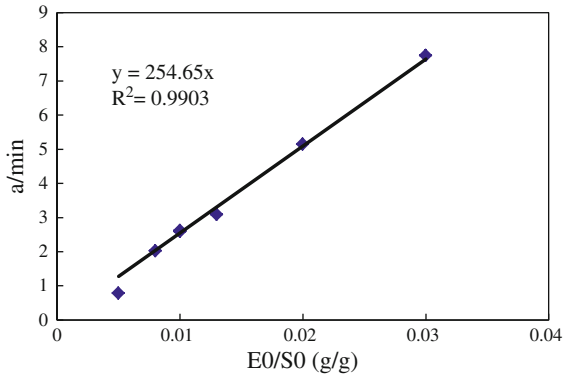

Fig. 9.16 Change trend of a value of Alcalase with different E_0/S_0 values

$$R = 254.65E_0 \exp[-0.3352(\mathrm{DH})] \tag{9.51}$$

It can be seen from Eq. 9.51 that the initial reaction rate of Alcalase enzymolysis peanut protein was only related to the initial Alcalase concentration and increased with the increase of initial Alcalase concentration. As the reaction progressed, the reaction rate decreased with the increase of degree of hydrolysis. After substituting the substrate concentration of 4% and the fitting result of logarithm model of Alcalase dosage of 2428 U/g into Eq. 9.51, the fitting curve of hydrolysis rate R and reaction time t were obtained.

It was shown from Fig. 9.17 that hydrolysis rate constantly decreased as enzymatic hydrolysis progressed, the reaction rate was only 0.733 at 120 min, and the reaction had been carried out very slowly.

Logarithm model was used to fit the data of Alcalase enzymolysis peanut protein by N120P, as shown in Table 9.11.

Based on Table 9.11 and Eqs. 9.41 and 9.42, the enzymolysis kinetics parameters a and b of Alcalase enzymolysis peanut protein by N120P were derived, as shown in Table 9.12.

From the results of Table 9.12, it was found that the change trend of enzymolysis kinetics parameters of Alcalase enzymolysis peanut protein by N120P was similar with that of Alcalase enzymolysis peanut protein. Among them are a decreased with the increase of initial substrate concentration and increased with the increase of

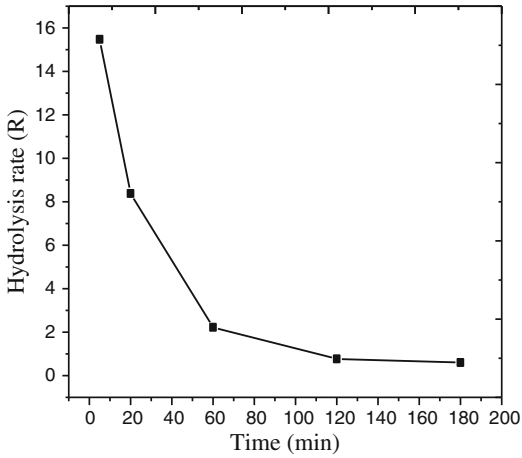

Fig. 9.17 Change of reaction range during Alcalase hydrolysis process

Table 9.11 Fitting results of logarithm model to N120P

Sample	Equation	Related coefficient
Substrate concentration 4%	$DH = -9.03114 + 3.78836^{*} \ln(t + 10.71919)$	0.9989
Substrate concentration 6%	$DH = -10.164 + 3.88376^{*} \ln(t + 13.45518)$	0.9989
Substrate concentration 8%	$DH = -10.06973 + 3.71547^{*} \ln(t + 14.64098)$	0.9964
Substrate concentration 10%	$DH = -11.04904 + 3.8058^{*} \ln(t + 11.04904)$	0.9944
Dosage of enzyme 600	$DH = -12.06741 + 3.86007^{*} \ln(t + 22.10365)$	0.9957
Dosage of enzyme 2400	$DH = -10.53295 + 3.86974^{*} \ln(t + 14.83674)$	0.9955
Dosage of enzyme 3600	$DH = -8.15434 + 3.7117^{*} \ln(t + 0.4125)$	0.9980

initial N120P concentration. The kinetics parameter b fluctuated up and down near its average value of 0.2629.

The linear fitting result of its a value and E_0/S_0 is shown in Fig. 9.18. The linear relationship formula $y = 9.46563x + 0.14519$, $R^2 = 0.9794$ obtained from Fig. 9.18 was consistent with Eq. 9.45, so the equation corresponding to the relationship curve of a value and E_0/S_0 value was:

$$a = 9.46563\frac{e_0}{S_0} + 0.14519 \tag{9.52}$$

In contrast to Eqs. 9.45 and 9.52, $K_2 = 9.46563$ (min^{-1}) was established.

After substituting the values of a and b into Eq. 9.38, the kinetics model of Alcalase enzymolysis peanut protein by N120P was established:

$$R = (9.46563E_0 + 0.14519)\exp[-0.2629(\text{DH})] \tag{9.53}$$

Table 9.12 Enzymolysis kinetics parameters by N120P

S_0(g/L)	E_0(g/L)	E_0/S_0(g/g)	a (min^{-1})	B
100	0.8	0.008	0.2087	0.2628
80	0.8	0.10	0.2472	0.2691
60	0.8	0.013	0.2836	0.2575
40	0.8	0.20	0.3492	0.2640
40	0.2	0.005	0.1694	0.2591
40	0.4	0.010	0.2544	0.2584
40	1.2	0.030	0.4125	0.2694

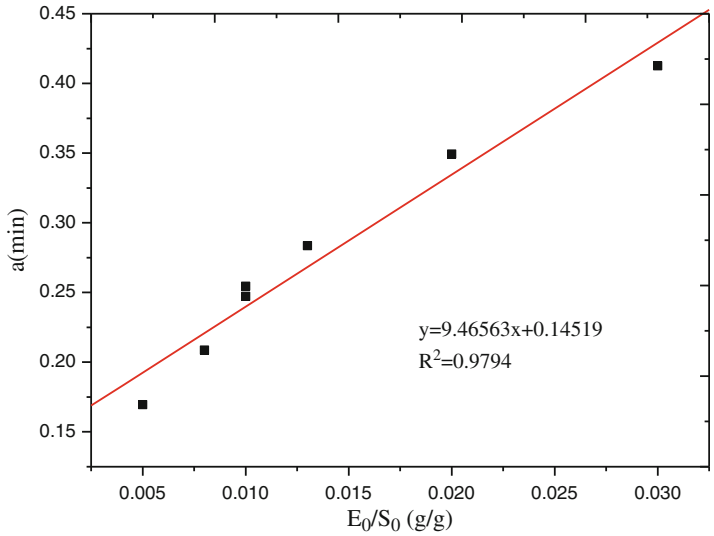

Fig. 9.18 Change trend of a value of N120P with different E_0/S_0 values

From Eqs. 9.64–9.53, it was shown that the hydrolysis reaction was still carried out when N120P was not added. At this time, the hydrolysis rate was very slow. With the addition of N120P, the reaction rate decreased with the increase of hydrolysis degree. After substituting the logarithm model fitting results when the substrate concentration was 4% and N120P dosage was 2400 U/g into Eq. 9.53, the fitting curve of hydrolysis rate R and reaction time t was obtained (Fig. 9.19).

It was shown in Fig. 9.19 that hydrolysis rate constantly decreased as enzymatic hydrolysis progressed, the reaction rate was only 1.1265 at 65 min, and the reaction proceeded very slowly.

3.2.3 Inactivation Constant of Protease

The activity of protease gradually decreased during the hydrolysis process, and the derivation and determination of the inactivation constant were helpful to explain the

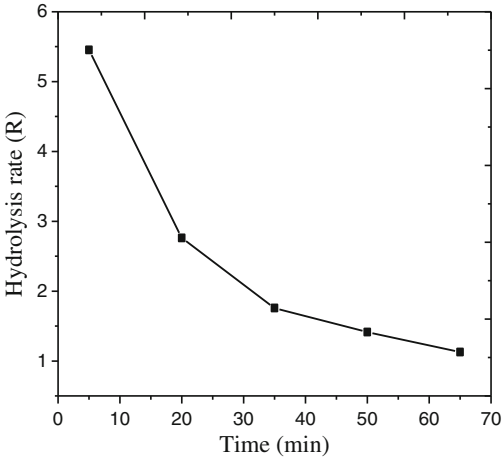

Fig. 9.19 Change of reaction rate during N120P hydrolysis process

role and inactivation of the protease in the hydrolysis process. Zhang Yuhao and Wang Qiang (2007) derived the kinetics parameters of the hydrolysis process of main tool enzyme Alcalase and auxiliary tool enzyme N120P during the preparation of peanut oligopeptide and established the corresponding kinetics model. The derivation results and process were as follows.

The following equation was established based on Eqs. 9.22, 9.26, and 9.29:

$$-\frac{\mathrm{d}e}{\mathrm{d}t} = K_d K_M \frac{e^2}{S_0} = K_4 \frac{e^2}{S_0} \tag{9.54}$$

where

$$K_4 = K_d K_M \tag{9.55}$$

K_4 was the Alcalase inactivation constant for the hydrolysis reaction.

After multiplying Eq. 9.37 with Eq. 9.38 and then merging with Eq. 9.55, the following equation was established:

$$ab = \frac{K_4 e_0}{S_0} \tag{9.56}$$

The ab value and the linear fitting results of E_0/S_0 were shown in Fig. 9.20.

The linear relationship formula $y = 84.777x$, $R^2 = 0.9908$ obtained from Fig. 9.20 was consistent with Eq. 9.36, so the equation corresponding to the relationship curve of ab value and E_0/S_0 value was:

$$ab = 84.777 \frac{E_0}{S_0} \tag{9.57}$$

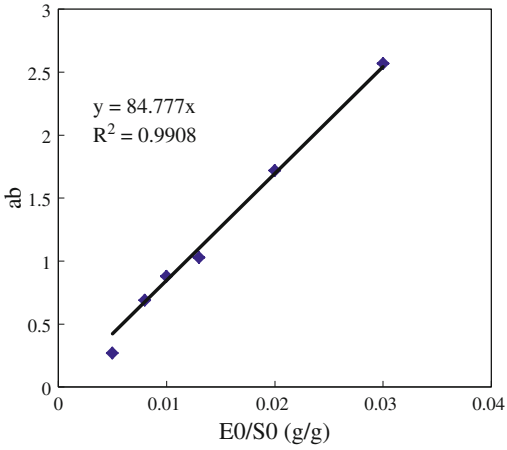

Fig. 9.20 Change trend of *ab* value of Alcalase with different E_0/S_0 values

In contrast with Eqs. 9.56 and 9.57, the kinetic constant of Alcalase inactivation was $K_4 = 84.777\ (\text{min}^{-1})$.

Multiplying Eqs. 9.45 and 9.38 and merging with Eq. 9.55, the following equation was established:

$$ab = \frac{K_4 e_0}{S_0} - K_4 c_0 \tag{9.58}$$

The linear fitting results of *ab* value and E_0/S_0 are shown in Fig. 9.21. The linear relationship formula $y = 2.60511x + 0.03675$, $R^2 = 0.98438$ obtained from Fig. 9.21 was consistent with Eq. 9.58, so the equation corresponding to the relationship curve of *ab* value and E_0/S_0 value was:

$$ab = 2.60511\frac{E_0}{S_0} + 0.03675 \tag{9.59}$$

In contrast with Eqs. 9.58 and 9.59, the kinetics constant of N120P inactivation was $K_4 = 2.60511\ (\text{min}^{-1})$.

3.2.4 Kinetics Model

The calculation results of enzyme kinetics model were compared with the actual hydrolysis results, to verify the practical application of the kinetics model. Therefore, the fitting between the hydrolysis degree curve of the system and the corresponding kinetics model calculation results was measured under a certain hydrolysis condition. Zhang Yuhao and Wang Qiang (2007) verified the kinetics model of the hydrolysis process of main tool enzyme Alcalase and auxiliary tool enzyme N120P during the preparation of peanut oligopeptide. The specific

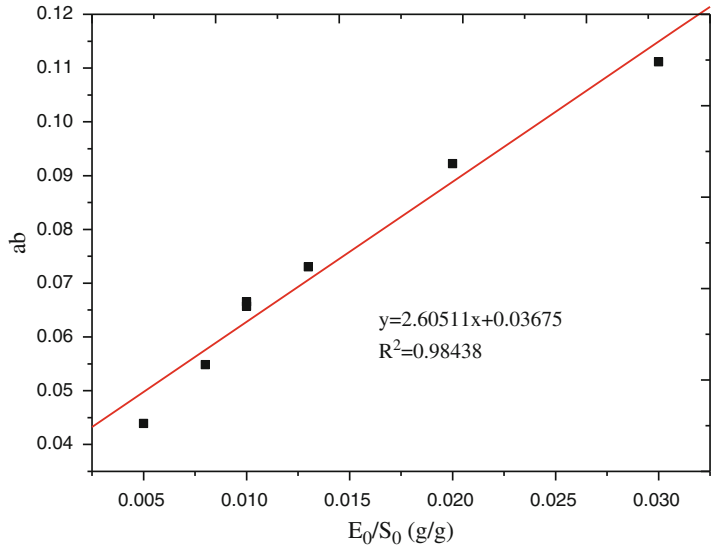

Fig. 9.21 Change trend of *ab* value of N120P with different E_0/S_0 values

conditions were as follows: initial substrate concentration of 4%, Alcalase dosage of 2428 U/g substrate, pH 8.0, reaction temperature of 53 °C, and reaction time of 105 min; later N120P continued to act on Alcalase, with dosage of 2400 U/g substrate, pH 6.0, reaction temperature of 57 °C, and reaction time of 65 min. As shown in Fig. 9.22, the model was well fitted and the error of most of the points was less than 5%, so the established kinetics model was credible.

3.3 Refining Classification

3.3.1 Desalination

During peanut protein hydrolysis process, it is required to adjust or maintain pH stability through acid-base regulation, so that peanut peptides contain a certain percentage of salt, while too high salt content will have a negative impact on product applications. Therefore, product quality should be improved by desalination process. The traditional desalting methods include ion exchange resin desalination method and macroporous resin method. The ion exchange resin method needs to exchange resin through anion and cation respectively, so that the desalination process is more cumbersome and the peptide recovery rate is low. This is because when the hydrolysate passes through the cation resin, the solution system is acidic, so that a large number of peptide molecules have positive charges in the solution, thus resulting in a large loss of peptide, and the result is the same when it passes through the anion resin. Macroporous resin method needs absorption and

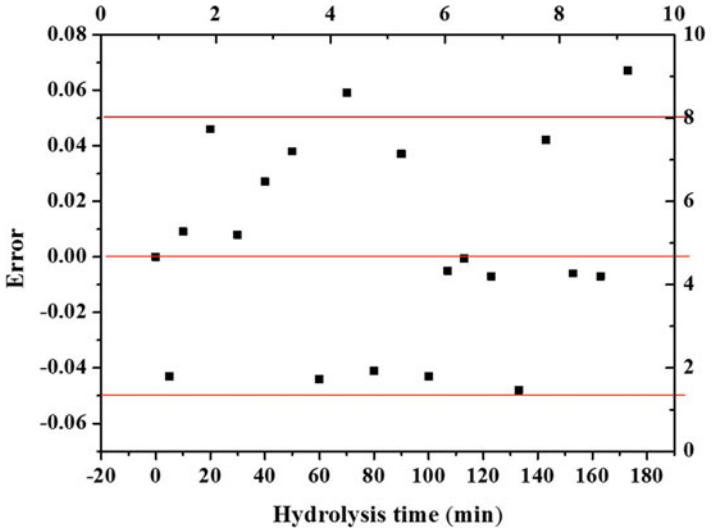

Fig. 9.22 Fitting of experimental hydrolysis degree and theoretical hydrolysis degree

elution process, so that the operation is tedious, the yield of peptide is low, and organic solvents need to be used during elution, and therefore it is not easy to achieve industrialization by this method.

Zhang Yuhao and Wang Qiang (2007) studied the desalting method of peanut peptides, established the mixed bed desalination method of anion and cation resins based on the traditional desalination method, and compared the processes of mixing bed, traditional ion exchange method, and macroporous resin method. The experimental results (Fig. 9.23) showed that during the peanut peptide desalination using mixed bed, both the desalination rate and oligopeptide yield were high. This was because during the desalination using traditional anion and cation resins, the entire solution system was acidic when hydrolysate passes through the cation resin, so that a large number of peptide molecules with positive charges were absorbed on the resin in the solution, and the result was the same when it passed through the anion resin. The other peptide molecules would be adsorbed on the pore size of the resin, so a great oligopeptide loss might be caused during desalination using anion and cation resins respectively. The pH of hydrolysate was stable during the desalination when using mixed bed, thus greatly reducing the loss of peptide during desalination; in addition, the interaction between the anions and cations could reduce the adsorption of resins to oligopeptide. It was shown that the desalination using mixed bed had obvious advantages in terms of oligopeptide yield compared with the other two methods.

Zhang Yuhao and Wang Qiang (2007) also optimized the factors in the desalination process using mixed bed. The results showed that the optimum conditions for the anion and cation exchange resin mixed bed desalination method were as follows: column passing speed of hydrolysate was five to ten times of column

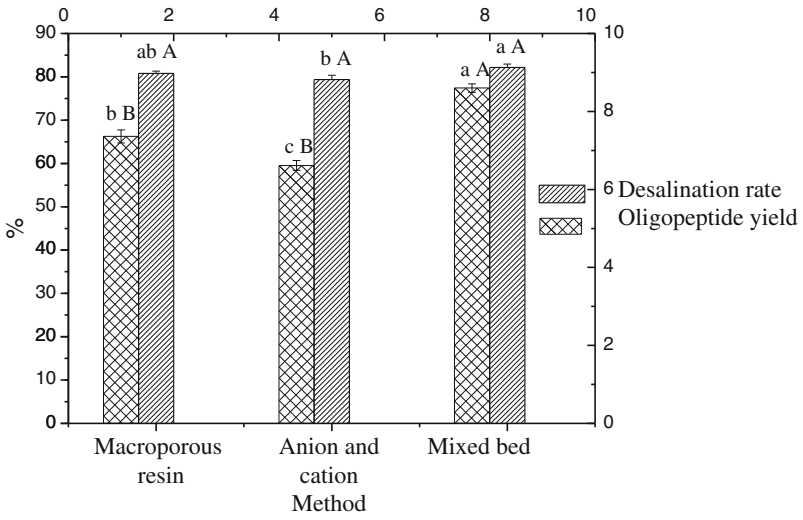

Fig. 9.23 Comparison of desalination method

volume/h, the pH value of hydrolysate was 4.5, and the ratio between anion and cation resins was 3:2. Under this condition, the desalination rate of peanut oligopeptide and protein recovery rate were all more than 80%.

3.3.2 Ultrafiltration

Peanut protein hydrolysates also contain some large molecular weight proteins, proteases, organic colloids, and other substances, which may limit their applications in the field of food, so it is required to conduct ultrafiltration classification for peanut oligopeptide. Ultrafiltration is the system to take the energy difference between the two sides of the membrane and realize heterogeneous system separation of the components in the solution due to the difference in particle size, with no interphase changes, low energy consumption, easy operation, small footprint, and other advantages. It is applied to the classification of protein hydrolysate, to realize the separation of polypeptides with different molecular weights. One of the major problems with ultrafiltration separation of protein hydrolysates is that membrane flux decreased with the extension of running time due to the impact of concentration polarization, membrane pore clogging, gel layer formation, and other factors. Therefore, it is very important for the long, safe, and stable running of ultrafiltration system as well as the increase of product yield to grasp and perform appropriate operating parameters.

3.3.2.1 Impact of Operation Pressure on Membrane Flux

The impact of operating pressure on ultrafiltration is mainly reflected in the formation of the gel layer on the membrane surface. Under a certain solute concentration and ultrafiltration temperature, appropriate operating pressure can delay the formation and thickening of the gel layer. During the ultrafiltration process, the greater the operating pressure is, the greater the pressure difference on both sides of the membrane is, and the greater the membrane flux is. However, as the ultrafiltration progresses, concentration polarization phenomenon may be caused at the membrane surface. The greater the operating pressure is, the more serious the phenomenon is. With the occurrence of concentration polarization, gel layer will be gradually formed at the membrane surface. The greater the operating pressure is, the thicker the formed gel layer is, the larger the mass transfer resistance is, and the smaller the initial membrane flux increase range is; therefore, when the operating pressure is too large, the thickness and density of gel layer formed during the ultrafiltration will increase correspondingly in addition to increasing energy consumption, thus resulting in reduced efficiency of ultrafiltration and serious ultrafiltration membrane pollution. However, too low ultrafiltration pressure might cause too low initial membrane flux, thus resulting in the low efficiency of the entire ultrafiltration process.

Zhang Yuhao and Wang Qiang (2007) conducted primary ultrafiltration to peanut oligopeptide using the ultrafiltration membrane with a molecular weight cutoff of 5000 Da and then conducted secondary ultrafiltration to the filtered solution using the ultrafiltration membrane with a molecular weight cutoff of 1000 Da. In this study, the impact of operating pressure on ultrafiltration effect was studied and explored (Figs. 9.24 and 9.25). The results showed that the optimum operating pressures for primary ultrafiltration and secondary ultrafiltration were 0.18 MPa and 0.21 MPa, respectively.

3.3.2.2 Impact of Feed Liquid Concentration on Membrane Flux

Protein and polypeptide are amphoteric compounds with strong surface activity, so they may be easily absorbed on the surface of polymer. Therefore, the impact of feed liquid concentration on ultrafiltration is mainly reflected in concentration polarization at the membrane surface and the formation of gel layer. Appropriate feed liquid concentration can allow more small-molecule solutes to pass through under the relatively small mass transfer resistance, thus improving the overall efficiency of ultrafiltration.

Zhang Yuhao and Wang Qiang (2007) studied and explored the impact of the feed liquid concentration on the ultrafiltration effect (Figs. 9.26 and 9.27) during the ultrafiltration process. The results showed that the optimum feed liquid concentrations for primary ultrafiltration and secondary ultrafiltration were 5–7.5% and about 7.5%, respectively.

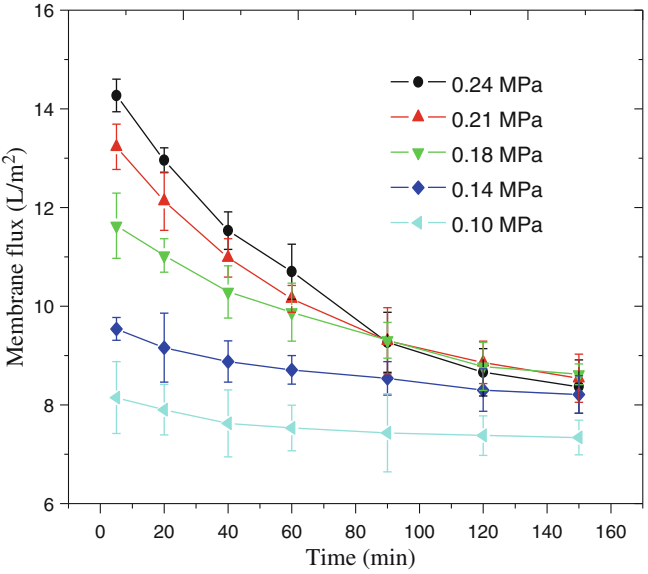

Fig. 9.24 Impact of operating pressure on primary ultrafiltration

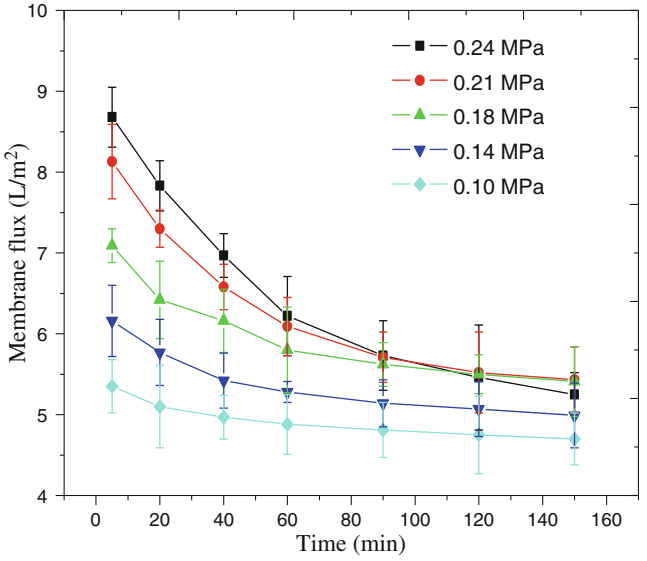

Fig. 9.25 Impact of operating pressure on secondary ultrafiltration

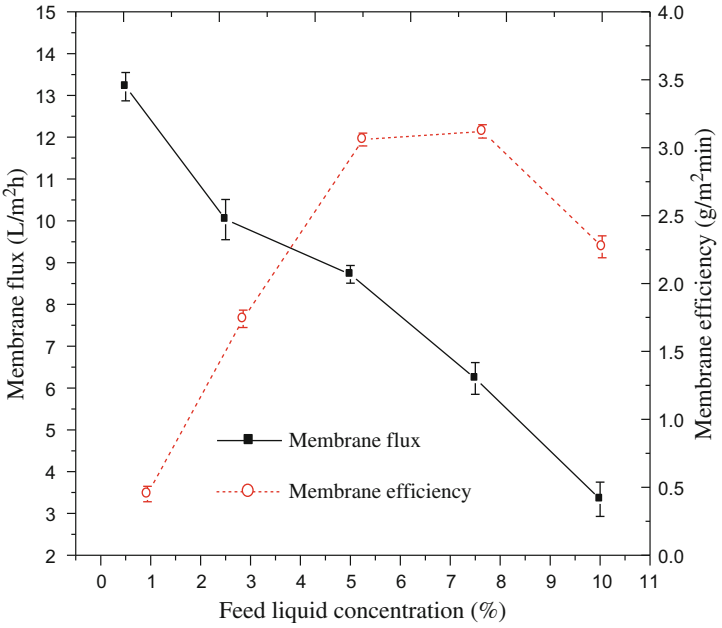

Fig. 9.26 Impact of feed liquid concentration on primary ultrafiltration

3.3.2.3 Impact of Operating Temperature on Membrane Flux

The impact of operating temperature on the ultrafiltration process is mainly reflected in its impact on feed liquid and then the impact on the polarization at the membrane surface. The increase of operating temperature might cause the viscosity of feed liquid to decrease and the diffusion coefficient to increase, which will reduce the impact of concentration polarization, so the membrane flux will increase with the rise of temperature. However, the adsorption of protein macromolecules on the membrane surface will increase with the rise of temperature, which will aggravate the contamination of membrane and rapidly reduce the increase range of membrane flux.

Zhang Yuhao and Wang Qiang (2007) studied and explored the impact of operating temperature on ultrafiltration effect during the ultrafiltration process (Figs. 9.28 and 9.29). The results showed that the optimum temperatures for primary ultrafiltration and secondary ultrafiltration were 35 °C and 40 °C, respectively.

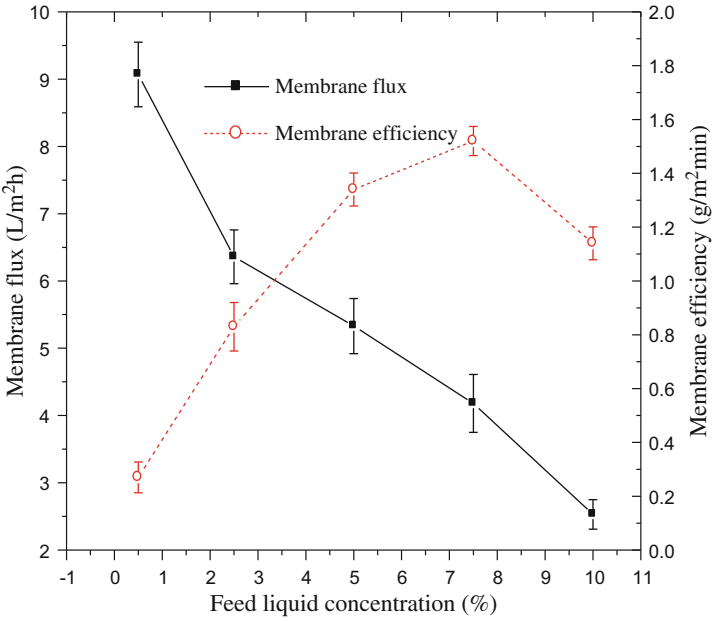

Fig. 9.27 Impact of feed liquid concentration on secondary ultrafiltration

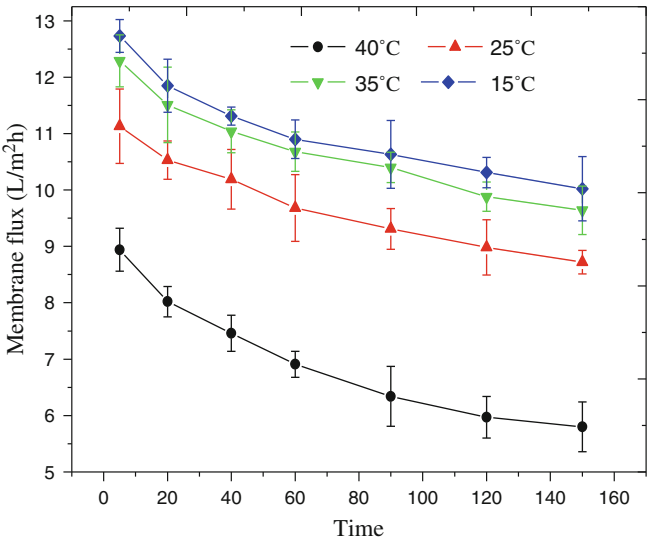

Fig. 9.28 Impact of operating temperature on primary ultrafiltration

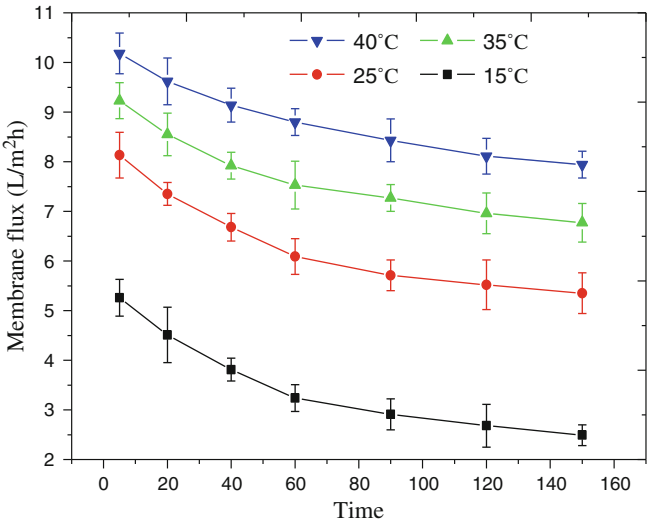

Fig. 9.29 Impact of operating temperature on secondary ultrafiltration

4 Evaluation of Biological Activity

Functional oligopeptides not only have a better absorption mechanism than that of amino acids but also have incomparable functional activity compared with a variety of amino acids. The relevant tests showed that the functional activity of oligopeptides mainly includes antihypertensive, antioxygenation, immune regulation, anti-thrombosis, and so on. In recent years, due to the insecurity of chemical antioxidant additives, the natural food antioxidants with high efficiency and low toxicity have become the current research focus; at the same time, due to the development of free radical life science, the functional foods and drugs with antioxidant function have also attracted the attention of many scholars. Studies (Shen Beiying 1996; Chen et al. 1995; Chen Meizhen et al. 2002) showed that the oligopeptides with molecular weight of about 1000 Da were effective free radical scavengers and antioxidants, because they could remove hydroxyl radicals, superoxide anion radicals, and other free radicals that were very harmful to the human body, prevent the damage to DNA due to excessive free radicals, and significantly prolong the life of rats and mice.

Since Cushman et al. (2002) derived the model of ACE active site according to the chemical structure of ACE substrate and designed the first chemically synthesized ACE inhibitor captopril based on this, synthetic ACE inhibitors have been generally recognized by the medical field. However, synthetic ACE inhibitors often tended to produce side effects in clinical applications, such as cough, taste dysfunction, and rashes (Chen Xiu et al. 2003). Therefore, it has attracted the great concern of the majority of scientific workers to look for ACE inhibitors from

natural and safe food sources to prevent and treat high blood pressure, and peanut oligopeptide is a natural blood pressure functional factor that meets this standard.

4.1 Antioxidant Activity

Jamdar et al. (2010) studied the antioxidant effects of peanut polypeptides. Studies showed that 2.0 mg/mL peanut peptide could reach DPPH free radicals by 50%, and the peanut peptide reduction force determination result of 10–40% peanut peptides with a hydrolysis degree of 2.5 mg/mL was between 0.72 and 0.98. It was also verified that peanut peptides had a certain ferrous ion chelating activity. Form this, peanut peptides had a strong action and reducing power to remove DPPH free radicals, but the antioxidant activity of peanut peptides was not compared with that of many antioxidant peptides.

Zhang Yuhao and Wang Qiang (2007) studied the antioxidant activity of desalinated peanut oligopeptide. The results showed that peanut oligopeptide had obvious antioxidant activity, and especially the activity of removing DPPH free radicals was strong. These results were the same as that of the study by Jamdar et al. (2010). However, compared with antioxidant peptides of soybean, the overall antioxidant effect of peanut peptides was not significant (Table 9.13). This might be related to the amino acid composition of peanut protein. In general, peptides with antioxidant activity contained histidine, methionine, and cysteine residues, which typically had a certain antioxidant activity in the free state with the ability to act as a nucleophile. Figure 9.30 listed the graphs of the chemical structures of histidine, methionine, and cysteine, respectively. It was shown from the figure that histidine molecule contained an imidazolyl group, which was both weak acid and weak base, so it was an excellent nucleophile with the ability to capture free radicals. Methionine and cysteine molecules contained sulfur atoms, among which methionine could capture hydroxyl radical and it was oxidized to methionine sulfone, thus playing an role in resisting oxidation and scavenging free radicals; sulfur in cysteine molecules existed in the form of sulfhydryl, and the molecules were polarizable, so it was a good nucleophile. Under the attack of reactive oxygen and other free radicals, sulfhydryl was oxidized to disulfide compound, and cysteine was oxidized to cystine.

Generally, the histidine, methionine, and cysteine contents in peanut protein are lower than that of soybean protein. This may be the reason why the antioxidant effect of peanut oligopeptide is not as good as that of soybean peptide.

4.2 ACE Inhibition and Antihypertensive Activity

Hypertension is an important risk factor for cardiovascular diseases such as heart failure, stroke, coronary heart disease, and myocardial infarction (Kannel 1996).

Table 9.13 Antioxidant activity of peanut oligopeptide

Implementation item	Concentration of peanut peptides (mg/ml)	Activity (%)	Concentration of soybean peptides (mg/ml)	Activity (%)
Superoxide radical	25	33.83 ± 3.31	25	41.70
Hydroxyl radical	15	62.15 ± 1.06	10	59.02
DPPH radical	10	71.60 ± 1.95	10	70.56
Ferrous ion chelating activity	50	40.01 ± 2.06	50	70.19

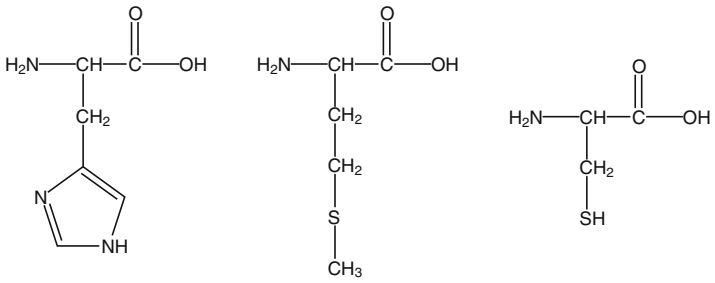

Fig. 9.30 Chemical structure graphs of histidine, methionine, and cysteine

Twelve million of people may die due to hypertension in the world. At present, the existing hypertensive patients in China have exceeded 120 million, so it is a very important issue to treat and prevent hypertension disease in today's society (Liu Lisheng 2001). Angiotensin-converting enzyme (ACE) plays an important role in the regulation of blood pressure in the human body; it participates in the regulation of blood pressure through renin-angiotensin system (RSA) and kallikrein-kinin system (KKS). RSA is a pressure increasing system that acts on angiotensin I by ACE and removes His-Leu from its end to generate angiotensin. As the strongest vasoconstrictor known in the RSA system, it acts on small arteries to shrink the vascular smooth muscle and rapidly cause pressure-increasing effect; meanwhile, angiotensin II can result in the increase of sodium storage and blood volume through stimulating aldosterone secretion and direct effect on the kidneys, thus increasing the blood pressure; on the contrary, KKS is a pressure-decreasing system, and it is also known as antihypertensive factor. Among them, kinin is an antihypertensive substance; ACE makes it lose the Phe-Arg and Ser-Pro at C-terminal by acting on soothing kinin in this system, thus degrading kinin into inactivation fragments and causing the elevation of blood pressure (Ondetti and Cushman 1977; Patchett et al. 1980).

Zhang Yuhao and Wang Qiang (2007) determined the ACE inhibition activity of peanut-mixed peptides after enzymolysis. The results showed that peanut oligopeptide ACE inhibited IC_{50} value to be 0.517 mg/ml and the mixed

antihypertensive peptide ACE inhibited IC_{50} value to be within the range of 0.126–246.7 mg/ml. It was shown that the inhibition activity of ACE of peanut oligopeptide was high. In recent years, Jamdar et al. (2010), Enyonam Quist et al. (2009), and Guang and Phillips (2009) have demonstrated that the functional peanut enzymolysis with high ACE activity can be prepared by the enzymatic hydrolysis of peanut protein.

4.2.1 Impact of Refining on the Inhibition Activity of ACE of Peanut Oligopeptide

4.2.1.1 Desalination

Oligopeptide is usually prepared by enzymolysis method of protein. During the enzymolysis process of peanut protein, in order to make the protease within the optimum pH range, it is required to maintain its hydrolysis rate as far as possible and add some alkali or acid to adjust the pH value of the hydrolysis system. Therefore, there is a certain amount of salt in the protein hydrolysate obtained finally, which may affect the purity and application scope of product and bring a negative impact on its functional activity, thus limiting its application in the food field. Therefore, desalination treatment should be conducted to peanut oligopeptide.

The desalination method of oligopeptide includes ion exchange method and macroporous resin method and nanofiltration treatment method. Nanofiltration is usually used as the pretreatment of ion exchange or macroporous resin to partially desalt polypeptides, so as to relieve the pressure of ion exchange resin or macroporous resin, and extend its saturation time. However, both macroporous resin treatment and ion exchange treatment may cause a certain degree of loss of oligopeptide. For example, ion exchange resin may cause the loss of oligopeptide rich in polar amino acids, and macroporous resin may cause the loss of oligopeptide rich in hydrophobic amino acid. Therefore, it is required to conduct a comprehensive assessment to the impact of desalination on the activity of oligopeptide.

Zhang Yuhao and Wang Qiang (2007) established the desalination method using mixed bed and evaluated the impact of desalination process on peanut oligopeptide ACE I activity. Studies showed that peanut oligopeptide ACE inhibited IC_{50} value to be 0.711 mg/ml before desalination and 0.517 mg/ml after desalination. It showed that the inhibition activity of peanut oligopeptide ACE increased after desalination, and the analysis of amino acid of peanut oligopeptide before and after desalination showed that the proportions of hydrophobic amino acids before and after desalination were 22.46% and 28.44%, respectively, indicating that desalination by mixed bed had enrichment effect on ACE I peptide to some extent. In addition, the purity of peanut peptides greatly increased after desalination, and the content of oligopeptide in the unit volume also increased, which was the cause why the ACE inhibition activity of peanut oligopeptide increased after desalination. It was found that the desalination by mixed bed was favorable to the preparation and enrichment of peanut ACE I oligopeptide.

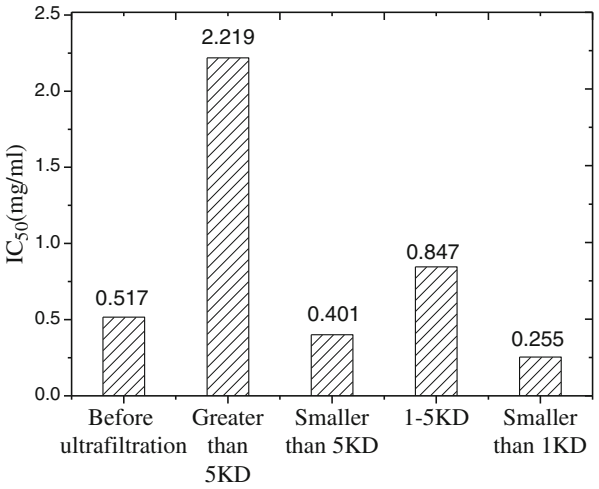

Fig. 9.31 Impact of ultrafiltration on the ACE inhibition activity of peanut oligopeptide

4.2.1.2 Ultrafiltration

Studies showed that most of the antihypertensive peptides were oligopeptides with a molecular weight of less than 1000 Da, so the peptide fragments with low molecular weight could be effectively enriched through ultrafiltration treatment. The studies of Zhang Yuhao and Wang Qiang (2007) showed that the ACE inhibition effect of the component with the molecular weight of less than 1000 Da in peanut oligopeptide after ultrafiltration separation was the best (Fig. 9.31), while the ACE inhibition activity of the component with the molecular weight of more than 5000 Da was the worst. The results showed that the ACE inhibition activity of peanut oligopeptide was closely related to its molecular weight, and ACE inhibition activity increased with the decrease of molecular weight, which was consistent with the previous study conclusions. Among them, the ACE inhibition activity of oligopeptide with the molecular weight of less than 1000 Da was especially prominent. Its IC_{50} could reach 0.255 mg/mL after ultrafiltration.

4.2.2 ACE Inhibition Activity Mechanism

4.2.2.1 ACE Inhibition Kinetics

Enzyme inhibition kinetics is the inhibition mode to establish enzyme kinetics model by investigating the relationship between the changes in substrate concentration and reaction rate under different inhibitor concentrations and thus judge the inhibition mode of the inhibitor. Enzyme inhibition mode is divided into irreversible inhibition and reversible inhibition; studies show that the inhibition of ACE

inhibitory peptide to ACE is reversible. Reversible inhibition is divided into three types:

Competitive inhibition: Inhibitor and substrate compete for the combination site of enzyme, thus affecting the normal combination of substrate and enzyme. The structure of most of the competitive inhibitors is similar with that of substrate, so it can combine with the active site of enzyme and form reversible EI compound with enzyme. However, EI compound cannot be decomposed into products, and thus the rate of enzyme reaction is reduced.

Noncompetitive inhibition: It is characterized by the fact that both the substrate and the inhibitor combined with the enzyme at the same time, both of which have no competitive effect. After the enzyme combines with the inhibitor, it can combine with substrate; after the enzyme combines with the substrate, it can combine with the inhibitor. However, the intermediate ternary compound cannot be further decomposed into products, resulting in reduced enzyme activity.

Uncompetitive inhibition: The enzyme can combine with the inhibitor only after combining with the substrate.

Zhang Yuhao and Wang Qiang (2007) studied the inhibitory kinetics of peanut oligopeptide with a molecular weight of less than 1000 Da. From Lineweaver-Burk (Fig. 9.32) model, it was found that the inhibition model of peanut oligopeptide to ACE was competitive inhibition, that is, peanut oligopeptide competed against substrate and combined with ACE active site to form a certain balance, thereby reducing the response rate of ACE to substrate. ACE inhibitory peptides in most of the reports were the competitive inhibitory peptides of ACE, and some peptides were the noncompetitive and uncompetitive inhibitors of ACE. For example, Saito et al. (1994) isolated ACE noncompetitive inhibitory peptides, while Nakagomi et al. (1998) prepared ACE uncompetitive inhibitory peptides from serum.

4.2.2.2 ACE Inhibitor Type

The premise for ACE inhibitory peptide to play a role in the human body after oral administration is that ACE inhibitory peptide can resist digestive enzyme hydrolysis and then be absorbed by the intestine in a complete form and go into the blood circulation and finally reach the target organ. Therefore, the ACE inhibition activity measured after simulating the digestive tract environment for the treatment of ACE inhibitory peptide is more close to the inhibition activity in human body. There are many reports on digestion test in vitro, and the difference in different study reports is mainly focused on the digestive enzyme species used, hydrolysis conditions, and product recovery and analysis methods. The best pH for digesting protein in the stomach by protease is 1–2; in the duodenum, trypsin, chymotrypsin, elastase, and carboxypeptidases A and B can continue to hydrolyze the protein in the best condition of pH 7–8. In the case of eating, the time for half emptying the food in the stomach is 0.5–3 h, the residence time in the duodenum and jejunum is 2–2.75 h, and the time in the ileum is 5–7 h.

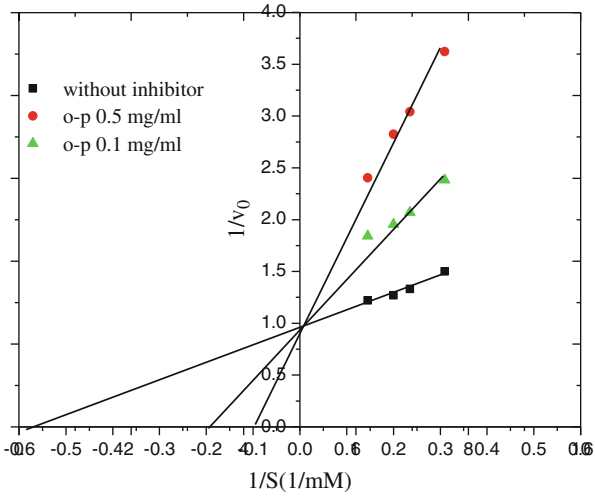

Fig. 9.32 Lineweaver-Burk model inhibited by peanut oligopeptide ACE

In order to investigate the resistance of protein hydrolysate to gastrointestinal digestive enzymes and the possibility of generating new ACE inhibitory peptides, further digestion treatment should be conducted to the peanut oligopeptide with the molecular weight of less than 1000 Da under the condition of simulating the physiological action of gastrointestinal digestion, to determine the changes in the ACE inhibition IC_{50} value of hydrolysate before and after digestion enzyme treatment and thus evaluate the digestion stability of hydrolysates. ACE inhibitory peptides can be divided into three types according to their digestion stability:

True inhibitor type: After in vitro intestinal enzyme simulation experiments, oligopeptide ACE inhibition activity is not affected.

Substrate type: After in vitro intestinal enzyme simulation experiments, oligopeptide ACE inhibition activity will decrease obviously.

Pro-drug type: After in vitro intestinal enzyme simulation experiments, oligopeptide ACE inhibition activity will increase obviously.

Zhang Yuhao and Wang Qiang (2007) studied the inhibition type of peanut oligopeptide with the molecular weight of less than 1000 Da. The results showed that peanut oligopeptide remained active after treatment with gastrointestinal digestive enzymes, indicating that peanut oligopeptide had a certain resistance to the hydrolysis of digestive enzyme. Therefore, peanut oligopeptide belonged to true ACE inhibitory peptide with true inhibition effect. This might be because peanut oligopeptide was less likely to be hydrolyzed by other proteases due to its low molecular weight. Therefore, the peanut oligopeptide with a molecular weight of less than 1000 Da could be absorbed into the blood circulation through the gastrointestinal tract in vivo, and functional peanut oligopeptide might play a role in lowering blood pressure after oral administration (Fig. 9.33).

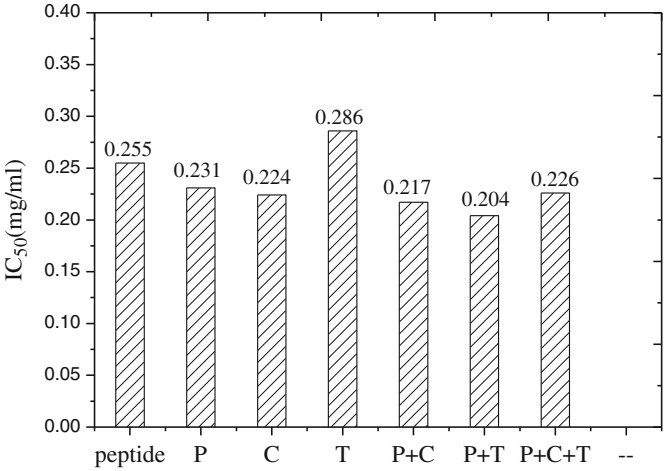

Fig. 9.33 Analysis of inhibition activity stability of peanut oligopeptide ACE (*Note*: *P* pepsase, *C* chymotrypsin, *T* trypsin)

4.2.3 Relationship Between Protein Amino Acid Composition and ACE Inhibitory Activity of Its Hydrolysates

At present, the studies on the ACE inhibitory peptides from food protein source are mainly focused on the optimization of enzymatic conditions, the isolation and purification of ACE inhibitory peptides, the structural characterization, and the in vivo activity test, while there are a small number of studies on the relationship between protein amino acid composition characteristics and ACE inhibitory activity. Zhang Yuhao and Wang Qiang (2007) collected the ACE inhibition IC_{50} value of some amino acid components from food protein source and their hydrolysates (Table 9.14) (Guanhong 2005; Wu and Ding 2002; Byun and Kim 2001), established the model between the amount of different types of amino acids and ACE inhibition IC_{50} value, and thus analyzed the relationship between amino acid species and protein hydrolysate ACE inhibition activity.

The scatter diagram of various amino acid contents and ACE inhibition activity is shown in Fig. 9.34. The regularity of aromatic amino acids was obvious; the regularity of hydrophobic amino acids and branched chain amino acids was relatively obvious, and only rice protein data were different from them; the alkaline amino acids, acidic amino acids, and amino acids without charges at side chains had large randomness in the scatter diagram, without any law; therefore, nonlinear fitting was conducted to hydrophobic amino acids, branched chain amino acids, aromatic amino acids, and ACE inhibition activity. Because rice protein data might affect the fitting of the regression function between hydrophobic amino acids and branched chain amino acids with ACE inhibition activity, this sample was removed when fitted. The results are shown in Figs. 9.35 and 9.36.

Table 9.14 Protein amino acid composition and its ACE inhibition activity

Amino acid	Peanut protein	Mung bean protein	Rice protein	Zein	Casein	Bovine serum albumin	Soybean protein	Collagen of *Gadus*
Asp	11.97	11.83	8.52	4.49	6.21	11.02	12.8	3.59
Glu	22.78	19.79	19.78	22.31	21.6	17.5	20.47	5.94
Ser	4.66	5.67	5.21	4.31	5.18	4.43	5.60	5.74
His	2.39	3.05	2.47	1.15	2.7	3.74	2.77	1.75
Gly	4.37	3.31	4.09	1.26	1.66	1.81	4.57	39.89
Thr	2.28	3.05	3.55	2.66	3.91	5.92	4.4	2.49
Ala	4.05	3.71	4.3	8.23	1.59	6.3	4.66	9.41
Arg	13.26	7.62	10.23	1.72	5.33	6.03	7.91	5.66
Tyr	4.05	2.97	5.74	5.1	5.36	5.45	3.43	0
Cys	0.68	0.26	0.8	0.8	0.21	6.38	1.45	0
Val	4.66	4.61	5.54	3.86	5.35	6.35	5.25	1.78
Met	1.3	1.26	2.76	2	3.37	0.9	1.38	1.43
Phe	5.79	6.45	5.84	6.85	5.16	6.71	5.41	1.36
Ile	4.01	3.54	3.8	4.15	3.95	2.76	4.97	1.2
Leu	7.07	8.28	8.54	17.3	8.47	12.05	7.81	1.99
Lys	3.04	7.12	3.25	0	6.8	12.98	6.98	1.96
Pro	3.63	4.51	4.87	9.19	8.76	4.85	6.01	9.38
Trp	0.87	1.21	1.58	1.01	1.41	0.61	0.93	0
Hyp	0	0	0	0	0	0	0	6.44
Hydrophobic amino acid[a]	35.43	36.54	42.97	57.69	43.42	45.98	39.85	26.55
Polar amino acid without charges at its side chain[b]	7.62	8.98	9.56	7.77	9.3	16.73	11.45	14.67
Basic amino acid[c]	18.69	17.79	15.95	2.87	14.83	22.75	17.66	9.37
Acidic amino acid[d]	34.75	31.62	28.3	26.8	27.81	28.52	33.27	9.53
Aromatic amino acid[e]	10.71	10.63	13.16	12.96	11.93	12.77	9.77	1.36

(continued)

Table 9.14 (continued)

Amino acid	Peanut protein	Mung bean protein	Rice protein	Zein	Casein	Bovine serum albumin	Soybean protein	Collagen of *Gadus*
Branched chain amino acid[f]	15.74	16.43	17.88	25.31	17.77	21.16	18.03	4.97
IC_{50}	0.71	0.62	0.14	0.27	0.46	0.39	0.54	0.84
$\lg\left(\frac{1}{IC50}\right)$	0.149	0.21	0.85	0.57	0.34	0.41	0.27	0.08

[a]Includes Ala, Ile, Leu, Met, Phe, Pro, Trp, Try, and Val
[b]Includes Ser, Thr, Cys, and Hyp
[c]Includes Lys, His, and Arg
[d]Includes Glu and Asp
[e]Includes Tyr, Phe, and Trp
[f]Includes Leu, Ile, and Val

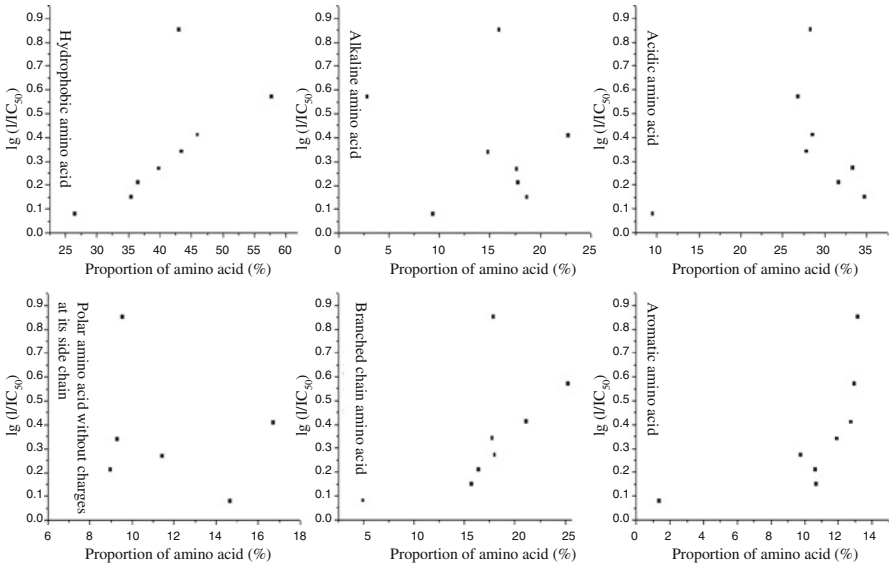

Fig. 9.34 Scatter diagram of amino acid content – ACE inhibition activity

The three fitting models of hydrophobic amino acid content and ACE inhibition activity of protein hydrolysate are shown in Fig. 9.35:

$$\text{Logistic model is}: y = -\frac{0.58}{1 + \left(\frac{x}{43.43}\right)^{7.11}} + 0.64 R^2 = 0.9945 \tag{9.60}$$

$$\text{ExpGro1 model is}: y = -2.52 + 2.2e^{\frac{x}{168.38}} R^2 = 0.9737 \tag{9.61}$$

$$\text{HyperbolaMod model is}: y = \frac{x}{-3.12x + 277.48} R^2 = 0.9188 \tag{9.62}$$

where x – proportion of hydrophobic amino acids in the protein:

$$y\text{—}\lg\left(\frac{1}{IC_{50}}\right) \tag{9.63}$$

The three fitting models of aromatic chain amino acid content and ACE inhibition activity of protein hydrolysate are shown in Fig. 9.36:

$$\text{ExpGro2 model is}: y = -0.06 + 9.3 \times 10^{-24} e^{\frac{x}{0.25}} + 0.02 e^{\frac{x}{4.98}} R^2 = 0.9653 \tag{9.64}$$

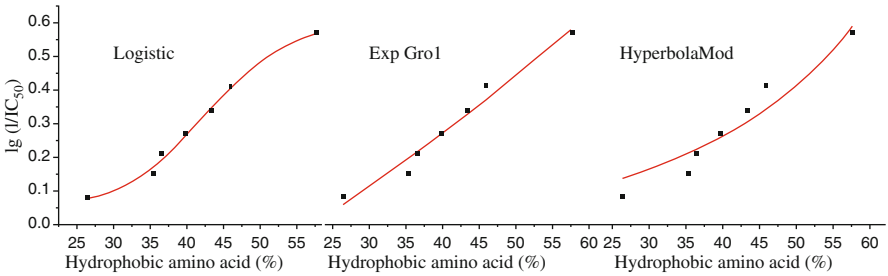

Fig. 9.35 Hydrophobic amino acid content – ACE inhibition activity model

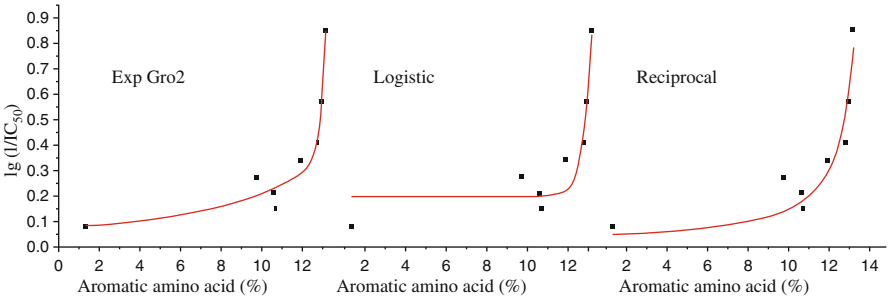

Fig. 9.36 Aromatic amino acid content – ACE inhibition activity model

$$\text{Logistic model is}: y = -\frac{3452.32}{1 + \left(\frac{x}{17.13}\right)^{32.6}} + 3452.5 R^2 = 0.9177 \tag{9.65}$$

$$\text{Reciprocal model is}: y = \frac{x}{24.01 - 1.73x} R^2 = 0.9107 \tag{9.66}$$

where x – proportion of aromatic chain amino acids in the protein:

$$y\text{—}\lg\left(\frac{1}{IC_{50}}\right) \tag{9.67}$$

The three fitting models of branched chain amino acid content and ACE inhibition activity of protein hydrolysate are shown in Fig. 9.37:

$$\text{Logistic model is}: y = -\frac{0.577}{1 + \left(\frac{x}{19.57}\right)^{6.54}} + 0.65 R^2 = 0.9600 \tag{9.68}$$

$$\text{Boltzmann model is}: y = -\frac{0.551}{1 + e^{\frac{x - 19.24}{2.76}}} + 0.62 R^2 = 0.9569 \tag{9.69}$$

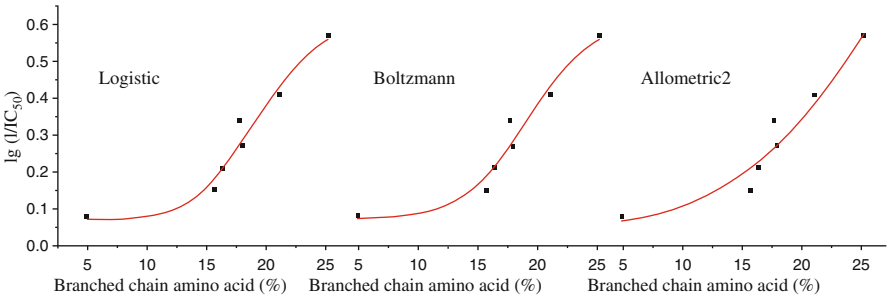

Fig. 9.37 Branched chain amino acid content – ACE inhibition activity model

$$\text{Allomentric 2 model is}: y = 0.06 + 0.00012x^{2.59} R^2 = 0.9385 \tag{9.70}$$

where x – proportion of branched chain amino acids in the protein:

$$y\text{—}\lg\left(\frac{1}{\text{IC50}}\right) \tag{9.71}$$

The three kinds of model fitting of Logistic, ExpGro1, and HyperbolaMod were conducted to hydrophobic amino acid content and ACE inhibition activity; the correlation coefficients of the three models established were greater than 0.9, indicating that the correlation of models was good. The trends reflected in the three models were basically consistent with each other, that is, the ACE inhibition activity of hydrolysate increased with the increase of hydrophobic amino acid content, indicating that the higher the hydrophobic amino acid content in the protein was, the higher the ACE inhibition activity of its hydrolysate was. The three kinds of model fitting of ExpGro2, Logistic, and Reciprocal were conducted to aromatic amino acid content and ACE inhibition activity. The model showed that high aromatic amino acid content was helpful to generating the oligopeptide with high ACE inhibition activity; however, different from hydrophobic amino acid, the ACE inhibition activity of hydrolysate would obviously increase with the increase of its content only when aromatic amino acid content was greater than 10%. The three kinds of model fitting of Logistic, Boltzmann, and Allometric 2 were conducted to branched chain amino acid content and ACE inhibition activity. The information reflected by the model was basically similar with that of hydrophobic amino acid, that is, branched chain amino acid content was positively correlated with the ACE inhibition activity of the hydrolysate.

The scatter diagram and nonlinear regression model showed that polar amino acid without charges at its side chain, basic amino acid, and acidic amino acid contents in the protein did not have any obvious impact on the ACE inhibition activity of protein hydrolysate; the increase of hydrophobic amino acid content, aromatic amino acid content, and branched chain amino acid content was helpful to increase the ACE inhibition activity of hydrolysate, that is, the protein with such

amino acid composition characteristics might generate a large amount of ACE inhibitory peptide with a high activity. Ruiz et al. (2004) considered that the impact of the content of Pro and Leu and their positions at oligopeptide C-terminal on ACE inhibition activity was large; Stevens et al. (2002) and Rohrbach et al. (1981) considered that when Pro was at the third position at C-terminal, the ACE inhibition activity of oligopeptide was high. Jung et al. (2006) considered that high-activity antihypertensive peptides contained a large amount of hydrophobic amino acids and aromatic amino acids, but the position of amino acid had a large impact on the ACE inhibition activity of oligopeptide. The ACE inhibition activity was stronger when the hydrophobic amino acids and aromatic amino acids of oligopeptide were at C-terminal. Other studies (Cheung et al. 1980) showed that when each position of tripeptide at C-terminal contained hydrophobic amino acid residues (aromatic or branched amino acid residues), it had a strong affinity with ACE; when there were aromatic amino acids and Pro at C-terminal of dipeptide or tripeptide and there were branched chain amino acid at N-terminal, it was more suitable for combination with ACE in a competitive inhibition manner. Thus, the conclusions of this study were consistent with previous studies. It was inferred from previous studies that although there is possibility of generating ACE inhibitory peptide from the amino acid composition characteristics of protein to a certain extent, the inner order of amino acids of protein also strongly affected the activity of ACE inhibitory peptides in addition to the composition of amino acids of protein, because ACE inhibitory peptide did not have a fixed structure. With the development of bioinformatics, more and more protein amino acid sequences have been elucidated, so it is helpful to select the protein material for the enzymatic preparation of ACE inhibitory peptides by combining the protein amino acid composition and sequence.

4.3 Antihypertensive Activity In Vivo

Based on the study of ACE inhibition activity in vitro, the hypotensive activity of oligopeptide usually requires further validation of their in vivo effects by animal experiments. Spontaneously hypertensive rats (SHR) are usually used as experimental animals, and the experimental process is usually divided into single dosing and multiple dosing experiments.

4.3.1 Antihypertensive Effect of Single Dosing

Zhang Yuhao and Wang Qiang (2007) studied the antihypertensive effect of single dosing for the peanut peptides with a molecular weight of less than 1000 Da. The results (Fig. 9.38) showed that after gavage to SHR for peanut oligopeptide and captopril with different dosages, the change trend of SBP of SHR was the group of peanut oligopeptide with low dosage remained antihypertensive activity within 1–7 h after gavage ($p < 0.05$), and the systolic blood pressure (SBP) of SHR

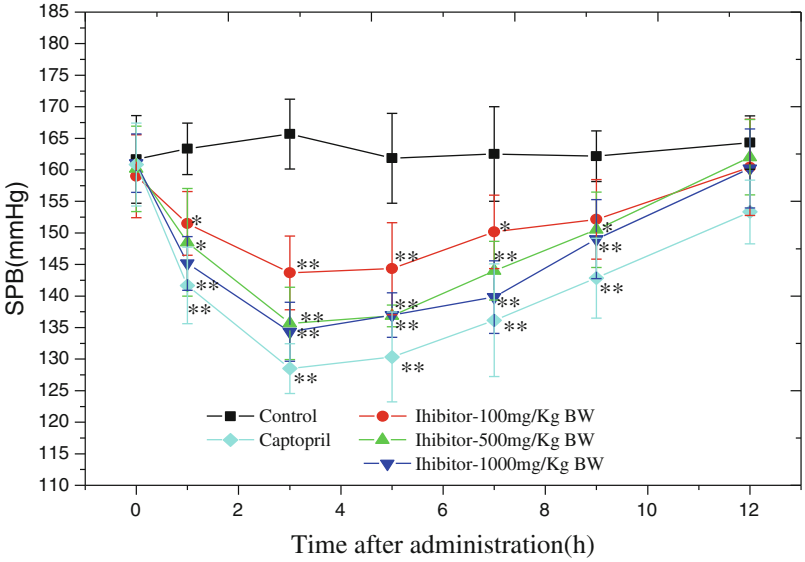

Fig. 9.38 Impact of single dosing on SBP of SHR

significantly decreased ($p < 0.05$) within 1–9 h after gavage in the group with medium and high dosages. The maximum decrease ranges of the three dosage groups all appeared 3 h after gavage, being 15.3 mmHg, 24.5 mmHg, and 26.8 mmHg, respectively. When the dosage of oligopeptide to SHR gavage was 500–1000 mg/ml, the maximum decrease range of SBP was 14–23 mmHg.

The studies on the changes in SHR heart rate after oral administration of peanut oligopeptide (Fig. 9.39) showed that there was no significant difference ($p > 0.05$) in the heart rate between all experimental groups and the control groups within 12 h and there was no significant difference ($p > 0.05$) between the experimental groups, indicating that peanut oligopeptide did not cause adverse impact on the circulatory system of SHR. Sigmoidal model (Fig. 9.40) was established using the maximum decrease range of SHR tail artery systolic pressure and oligopeptide dosage in the groups with different dosages, and the following equation was established:

$$Y = \frac{42.206}{1 + e^{\frac{x+0.43325}{0.5046}}} - 25.654, R^2 = 0.9955 \tag{9.72}$$

This showed that the maximum decrease range of SHR tail artery systolic pressure tended to a fixed value with the increase of dosage of peanut peptide, rather than increasing with the increase of dosage of peanut peptide, so hypotension phenomenon would not be caused due to dosage deviation in the actual applications. The study results showed that peanut antihypertensive peptides had hypotensive effect on hypertensive rats or patients and the hypotensive effect was smooth,

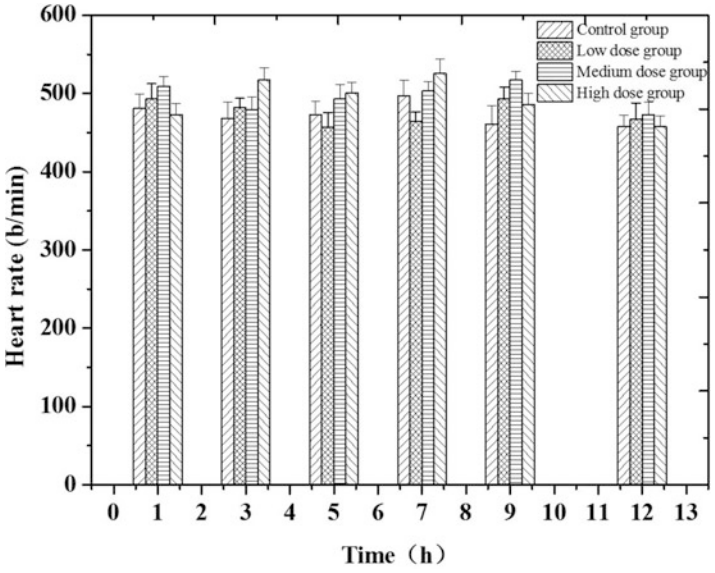

Fig. 9.39 Impact of peanut oligopeptide on SHR heart rate

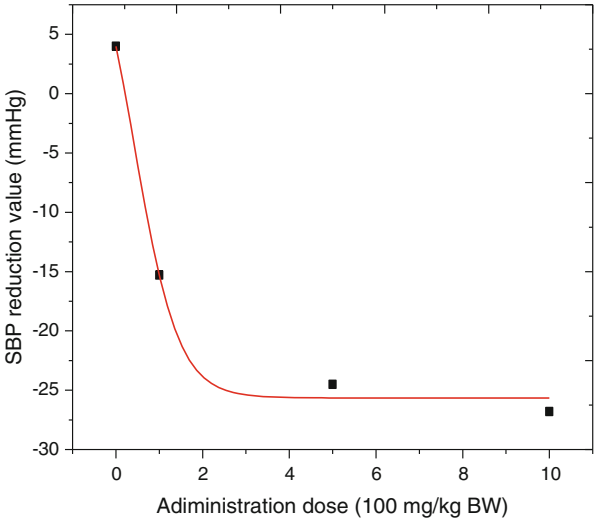

Fig. 9.40 Dose-effect sigmoidal model of peanut oligopeptide

but it did not have any impact on the ones with normal blood pressure; therefore, it was safe without any side effects.

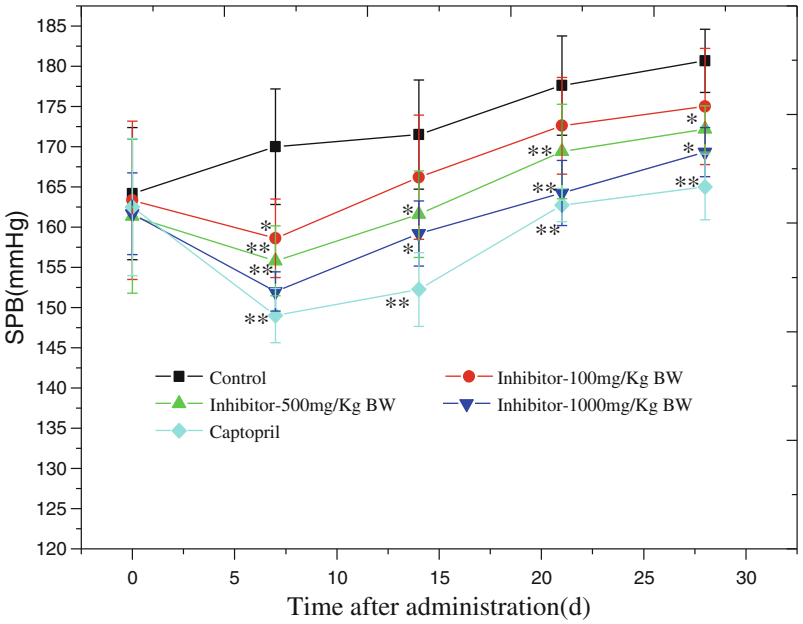

Fig. 9.41 Impact of repeated administrations of peanut oligopeptide on SBP of SHR

4.3.2 Antihypertensive Effect After Repeated Administrations

Zhang Yuhao and Wang Qiang (2007) studied the antihypertensive effect of peanut peptide with a molecular weight of less than 1000 Da after repeated administrations (Fig. 9.41). The results showed that the gavage administration of peanut oligopeptide with different dosages had different degrees of antihypertensive effects on SHR. The SBP of SHR in the three oligopeptide groups decreased by 11.4–18 mmHg 1 week after administration, with significant difference ($p < 0.05$) compared with that of blank group, and later the SBP of the dosage groups rose with the extension of time, because its SBP would rise with the increase of rat age of SHR. Within 4 weeks, the SBPs of medium- and high-dosage groups were significantly lower than the blank group ($p < 0.05$), indicating that long-term blood pressure reduction would be achieved after administration of the peanut oligopeptide with a dosage of 500 mg/kg BW and above.

Studies showed that small peptides and even oligopeptides above tetrapeptide were easily absorbed into the blood circulation in a complete form, the peptide vector genes of mammalian and human had been cloned and expressed, and it was verified that there were two peptide carriers in vivo. After oral administration of yogurt containing ACE inhibitory peptide Ile-Pro-Pro and Val-Pro-Pro, SHR blood pressure was significantly reduced, and at the same time the ACE activity of aorta abdominalis was significantly inhibited, and these two kinds of peptides were tested in the aorta abdominalis.

Table 9.15 Determination of ACE activity in the serum of SHR after repeated administration ($p = 0.05$)

Sample	ACE activity of plasma blood (AU)	Sample	ACE activity of plasma blood (AU)
Blank	30.58 ± 1.96	500 mg/kg BW	24.06 ± 3.05*
100 mg/kg BW	25.71 ± 2.41	1000 mg/kg BW	22.69 ± 1.36*
		Catropril	17.01 ± 2.62**

The studies of Matsui et al. (1999) demonstrated that ACE inhibitory peptide Val-Tyr ($IC_{50} = 26$ μM) could be fully absorbed in the blood of persons with normal blood pressure and hypertensive patients. Vermeirssen et al. (2002) found that the ACE inhibitory peptide Ala-Leu-Pro-Met-His-Ile-Arg could completely be transported from mucosal layer to the other side from β-lactoglobulin using the study on Caco-2 single cell layer. Zhang Yuhao and Wang Qiang (2007) determined the ACE activity in the serum of SHR after repeated administration, and the results (Table 9.15) showed that the ACE activities in the serum of SHR in the groups with medium and high dosages were significantly lowered than that of the blank group ($p < 0.05$). It proved that peanut peptides could be completely absorbed into the blood circulation and thus produce hypotensive activity.

The study results of Zhang Yuhao and Wang Qiang (2007) showed that in both single administration experiment and multiple administration experiment, the antihypertensive effect of captopril was better than that of peanut oligopeptide. However, it is well known that chemically synthesized antihypertensive drugs have obvious side effects such as the toxic and side effects of the kidneys and other side effects such as hypotension and dry cough. The study results showed that peanut oligopeptide was ACE inhibitor from natural and safe food sources. Therefore, peanut oligopeptide can be used as a new functional food for the prevention and control of hypertension.

5 Structural Characterizations and Structure-Function Relationship of ACE Inhibitory Peptide

The separation and purification of oligopeptide are the processes to enrich, purify, and identify the oligopeptide by using gel chromatography, ion exchange chromatography, HPLC, and HPLC-MS and taking a specific functional activity as the evaluation indicator. Gel filtration chromatography is a chromatographic method for achieving the separation effect according to the different molecular weights of the separated substances. The filler used in the gel filtration chromatography is a material having a three-dimensional network structure with a uniform diameter in bead-like particles. When a mixture solution containing different molecular weights is passing through a gel column, the buffer solution and small and large molecular

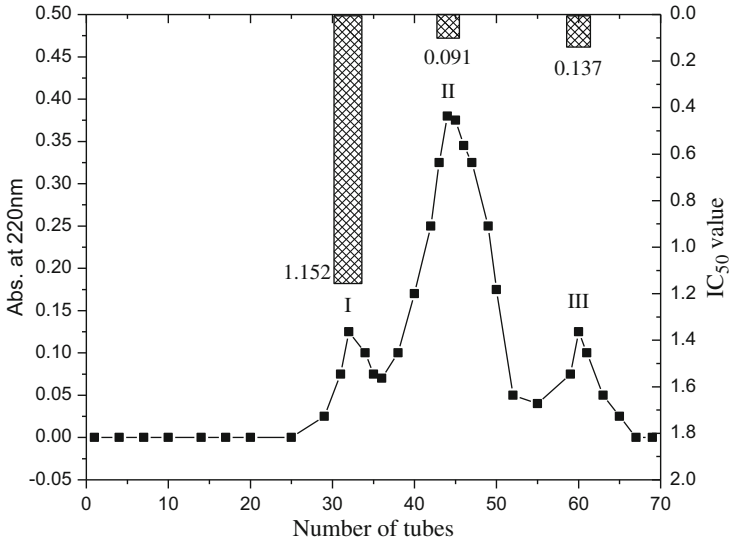

Fig. 9.42 Gel filtration separation of peanut oligopeptide

compounds are able to freely spread and penetrate in the sieve pores, while macromolecular substances are blocked outside the sieve pores. Therefore, the substances with high molecular weight flows in the gap of filler particles, so they can be eluted earlier than the substances with low molecular weight.

5.1 Gel Filtration Separation

The author's study group (2007) conducted gel chromatography separation to peanut ACE I peptides using Sephadex G-15. The results showed that the peanut oligopeptide with a molecular weight of less than 1000 Da could be separated into three peaks (Fig. 9.42), among which the hypotensive activity of peak 2 (PP-II) was the strongest and its IC_{50} value could reach 0.091 mg/ml.

5.2 Separation of PP-II by Semi-preparative RP-HPLC

RP-HPLC principle is to separate the samples according to different molecular polarities of components. Due to such advantages as high resolution, fast analysis speed, and high product recovery, it has become one of the most effective means for the separation and preparation and analysis of polypeptide substances. Peptide component PP-II automatically collected 27 major components after separation by semi-preparative RP-HPLC, as shown in Fig. 9.43. After repetitive sample

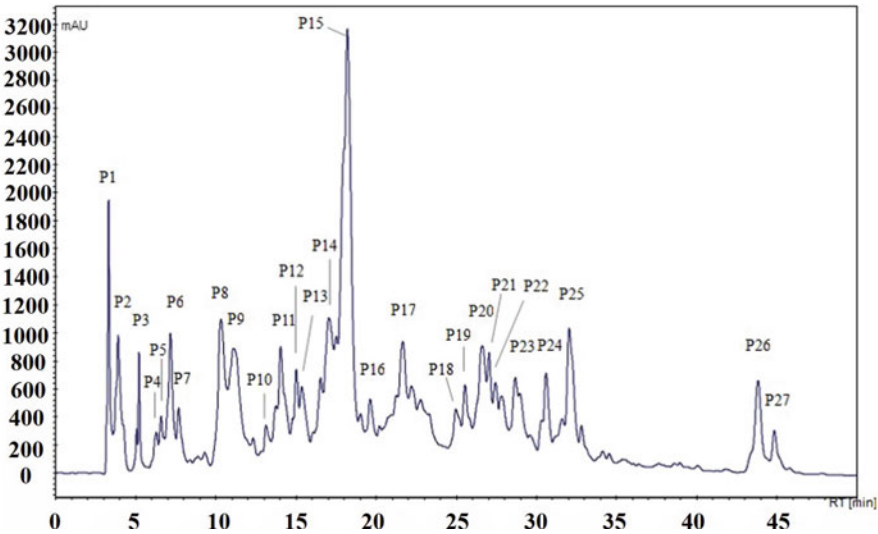

Fig. 9.43 PP-II graph of peanut peptides separated and purified by semi-preparative RP-HPLC

introduction, the peptide concentration of 0.010 mg/mL was prepared by merging the same components obtained each time and then freezing and drying it, and then dissolving it into the distilled water, to determine the ACE inhibition activity of components, as shown in Fig. 9.44. It was shown that the activity of component 8 (recorded as P8) was strong, and the ACE inhibition range reached $85.77 \pm 3.95\%$, followed by P3 and P11, the ACE inhibition ranges of which were $66.79 \pm 2.00\%$ and $66.15 \pm 2.11\%$, respectively. Therefore, component P8 was selected for structural identification. Chromatographic column, Varian C18 (21.2×150 mm); column temperature, 25 °C; flow rate, 10 mL/min; detection wavelength, 280 nm; sample introduction sample, 1 mL; elution condition, 0–50 min, 95%–70% A, 5–30% B (A, water +0.05% TFA; B, acetonitrile +0.05% TFA).

5.3 Purity Identification of P8 After Purification

To examine the RP-HPLC separation effect described above, the author's study group conducted purity identification to P8 component. It was shown from Fig. 9.45 that there was a single peak in the RP-HPLC graph of P8, indicating that P8 component might contain only one peptide fragment, and the next step could be conducted for structural analysis. Chromatographic column, C_{18} column (4.6×250 mm); flow rate, 0.5 mL/min; detection wavelength, 280 nm; sample introduction sample, 20 μL; column temperature, 30 °C; elution condition,

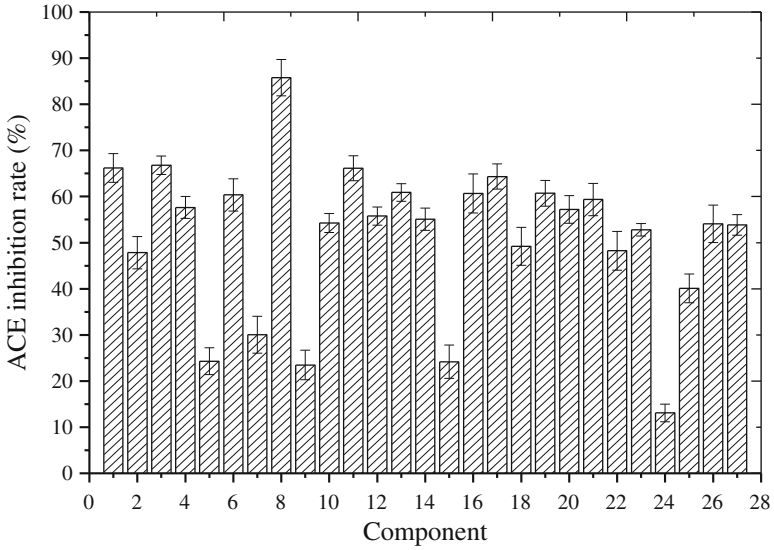

Fig. 9.44 ACE inhibition rates of PP-II components of peanut peptides separated and purified by semi-preparative RP-HPLC

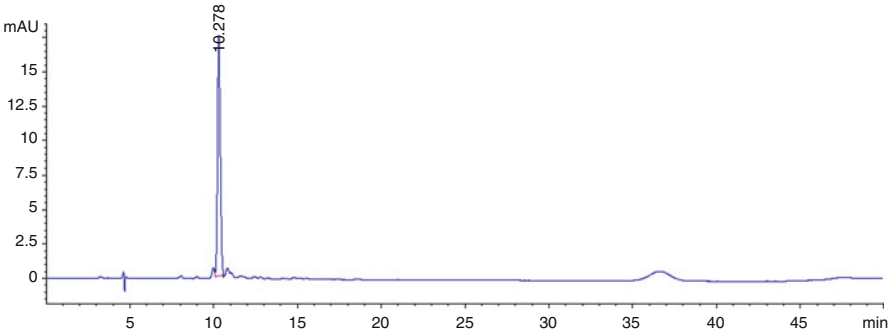

Fig. 9.45 RP-HPLC analysis graph of P8 after purification

0–20 min, 95–70 % A, 5–30 % B (A, water +0.05% TFA; B, acetonitrile +0.05% TFA).

5.4 Analysis of Amino Acid Sequence of ACE Inhibitory Peptide Using MALDI-TOF-TOF

The traditional sequencing methods for peptide and protein analysis include enzymolysis method at C-terminal, Edman degradation method, and DNA

translation method. These methods have some shortcomings: for example, as the standard method for determining peptide and protein sequences, N-terminal Edman method (also known as PTH method) has such shortcomings as high requirement for the purity of sample, large consumption amount of sample, and slow sequencing speed; due to incorrect identification to modified amino acid residues, it cannot conduct sequencing for peptide chain with N-terminal protection; it is difficult to find the ideal chemical probe by C-terminal chemical degradation sequencing method (Liao Dan-kui et al. 2006). Mass spectrometry features high sensitivity, accuracy as well as easy operation, and fast speed. With the appearance of FAB, ESI, MALDI, and other soft ionization methods, its applications in biological field have developed rapidly. MALDI-TOF-TOF can be used directly to determine the amino acid sequence of the peptide. The parent ions of peptide fragment generated at primary mass spectrum will selectively enter secondary mass spectrum, the peptide fragments will be broken along the peptide chain after collision against the inert gas, and the mass difference value of the peptide fragment obtained will be used for deducing the peptide sequence.

The tandem mass spectrometry data obtained can be used to analyze peptide sequence from the beginning using software, or it can combine with amino acid analysis to obtain the sequence results by manual analysis. The breakage of peptide follows a certain rule, and the general peptide breakage mode and fragment type are shown in Fig. 9.46 (Guo Hongying 2009). N-terminal series of fragment ions (b series) and C-terminal series of fragment ions (y series) will be obtained after the breakage of peptide bond. These fragments can further form dehydrated and deaminized ions.

MALDI-TOF-TOF analysis (4700 Proteomics Analyzer mass spectrometer) was conducted to peanut oligopeptide component P8, and secondary mass spectrum analysis was conducted to the fragmented ions of parent ions to obtain MS/MS graph (Fig. 9.47). In MS graph, the peak ($m/z = 810.8$) was molecular ion peak $[M + 2H]^{2+}$, and the molecular weight of component P8 was 808.8 (theoretical relative molecular weight was 808.7). In the analysis using software, the amino acid sequence of P8 was Lys-Leu-Tyr-Met-Arg-Pro. IC_{50} value was 0.0052 mg/mL (6.42 μM) in the determination of ACE inhibition activity of component P8 (Table 9.16).

5.5 *Verification of ACE Inhibition Activity of Synthetic Oligopeptide KLYMRP*

In order to further verify the functional activity of peanut hexapeptide Lys-Leu-Tyr-Met-Arg-Pro (KLYMRP), the oligopeptide with the same amino acid sequence was synthesized by solid-phase synthesis method, and ACE inhibition IC_{50} value was 0.0038 mg/mL (4.69 μM) in the determination of activity of synthetic peptide. Experiments showed that the oligopeptide with such amino acid sequence had

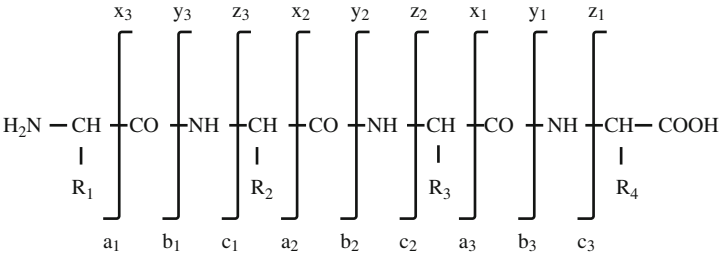

Fig. 9.46 Peptide skeleton breakage and naming of its fragment ions

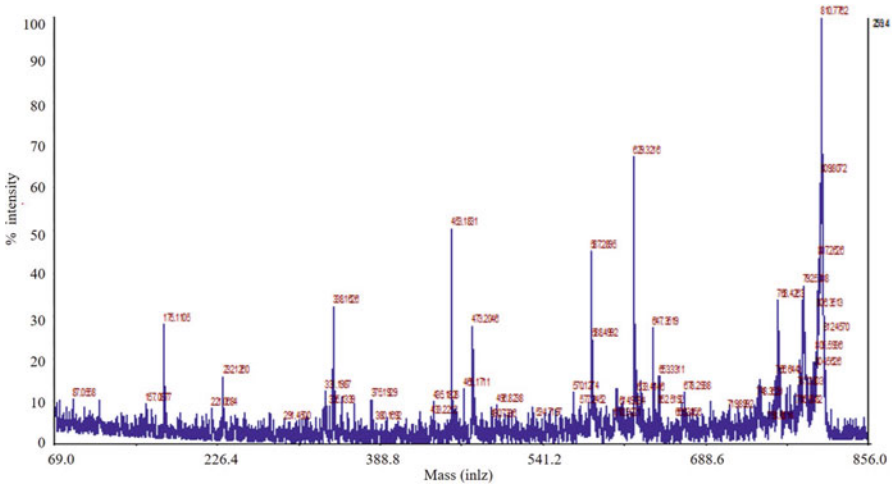

Fig. 9.47 MALDI MS/MS graph of oligopeptide P8

Table 9.16 Amino acid sequence and activity of peanut ACE inhibitory peptide

Peanut ACE inhibitory peptide P8	Analysis results
Theoretical relative molecular weight	807.7
Measured mass spectrum mass	808.8
Amino acid sequence	Lys-Leu-Tyr-Met-Arg-Pro
IC_{50}	0.0052 mg/mL (6.42 μM)

in vitro ACE inhibition activity, and the activity of synthetic peptide was higher than that of oligopeptide KLYMRP from peanut protein source.

5.6 *Structure-Activity Relationship of Oligopeptide KLYMRP*

The most stable molecular conformation of high-activity ACE inhibitory peptide P8 was specified by computer simulation method (Discovery Studio, Accelrys). It would have different activities due to the transition of the tertiary structure of oligopeptide based on the conformation when it played a role in antihypertensive activity after docking with ACE.

5.6.1 Conformation Optimization of Oligopeptide KLYMRP

Molecular dynamics has been widely used in the field of life sciences, such as the study on the mechanism of protein folding, study on the mechanism of enzyme catalysis reaction, study on the movement of function-related proteins, and study on the large-scale conformational changes of biological macromolecules, so it has become one of the essential methods in the study on theoretical biology.

Oligopeptide chain initial structure was constructed according to the amino acid sequence of oligopeptide P8 (KLYMRP). Conformation optimization was conducted through molecular dynamics simulation. The main steps included pretreatment, giving position, adding solvent environment, temperature rise, equilibrium, and sampling. The lowest potential energy conformation was searched and analyzed, that is, the most stable molecular conformation of the oligopeptide would be used for subsequent molecular docking link. Figure 9.48 showed the most stable molecular conformation (pH 7.4, 300 K) of oligopeptide after 200S of kinetics simulation under the position of CHARMm, and the distance from its C-terminal and N-terminal was 9.448 Å.

5.6.2 Analysis of the Interaction Between Oligopeptide KLYMRP and ACE

The interaction between oligopeptide and ACE was analyzed using molecular docking technique. This technology is to place ligand molecules at the position of active site of receptor molecule; evaluate the interaction between the ligand and the receptor in real time according to the principle of geometry complementarity, energy complementarity, and chemical environment complementarity; and then find the best combination mode between the two molecules. Angiotensin-converting enzyme (ACE) plays an important role in regulating blood pressure, electrolyte and body fluid balance, cardiovascular system development, and structural remodeling, and its inhibitors have been successfully used as first-line drugs for the treatment of hypertension. Oligopeptide can have different activities due to the transformation of the tertiary structure by using oligopeptide KLYMRP as a

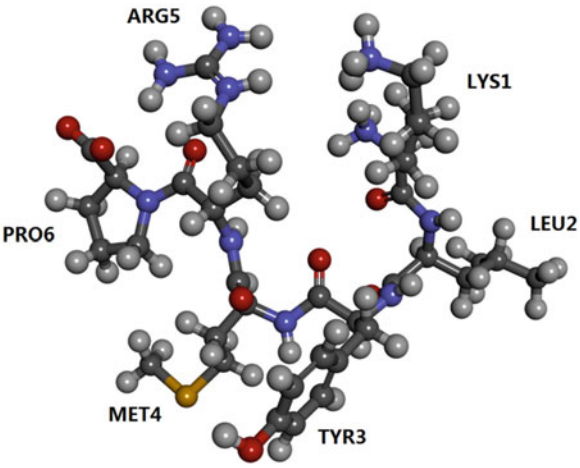

Fig. 9.48 Most stable molecular conformation of oligopeptide KLYMRP

ligand molecule in the active site of the receptor molecule ACE and studying the interaction between this oligopeptide and ACE.

The module of DS_CDOCKER was used for molecular docking. Among them, ACE protein structure came from PDB database (the code was 1UZE), the docking receptor was obtained by removing the ligand (EAL3002) and water molecules in this structure, and the ligand was the oligopeptide molecule KLYMRP after optimization by kinetics model, while the active sites of receptor during docking were obtained using "active pocket search" in DS3.5 software. After the assessment on the docking results using CDocker Energy, CDocker Interaction Energy, LibDockScore, and other scoring functions, the optimal docking compound conformation at pH 7.4 and 300 K was obtained (Fig. 9.49). It was clearly shown from the conformation of this compound that oligopeptide KLYMRP could act well in the "active pocket search" of ACE and then form a variety of interaction with its amino acid residues (Douglas and Sturrock 2012).

Figure 9.50 showed the interaction between oligopeptide KLYMRP and amino acid residues in ACE. There were many hydrogen bond acceptors and donors at the surface of oligopeptide KLYMRP, and these structures were helpful to form stable KLYMRP-ACE compound during the interaction with ACE. The main force formed by KLYMRP and ACE residues is shown in Fig. 9.51. The results showed that KLYMRP and ACE mainly formed three kinds of forces, including hydrogen bond force, electrostatic force, and Pi bond force, and the main ACE amino acid residues that formed these forces included 403-, 123-, and 143-bit glutamic acids, 355- and 517-bit serine, and 124-bit arginine. Glutamic acid is a kind of acidic amino acid with two carboxyls, and it is easily used as the proton receptor to form hydrogen bonds; serine is the amino acid that takes hydroxyl as side chain, and it can be used as both proton donor and proton receptor due to small space occupation; arginine contains a guanidyl; this group has a strong positive charge, so it can be used as a proton donor to form hydrogen bonds. In KLYMRP, LYS1, ARG5, and

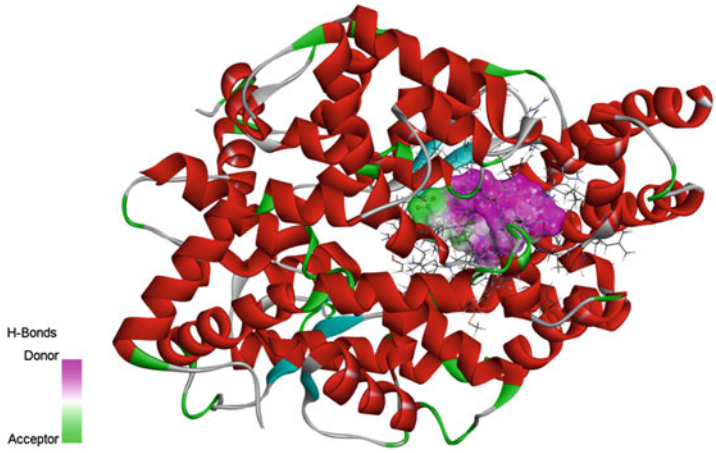

Fig. 9.49 Oligopeptide KLYMRP-ACE compound conformation with the highest scores in CDocker Energy

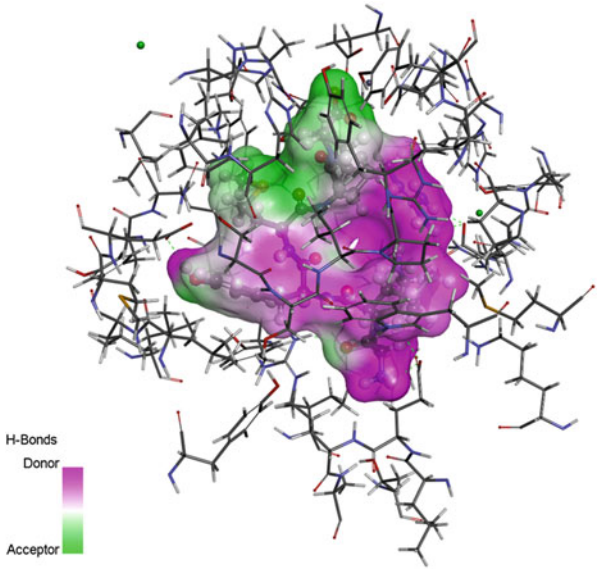

Fig. 9.50 Interaction between oligopeptide KLYMRP and ACE amino acid residues

PRO6 are the main action sites, the polarity and space size of side chain are the main factors to form these action force.

Table 9.17 listed the bond length and force size of oligopeptide KLYMRP and the main interactive groups of ACE. Among them, the glutamic acid residues on ACE and oligopeptide KLYMRP had the strongest interaction force, being −143.2075 kcal/mol; the interaction between arginine at ACE and oligopeptide

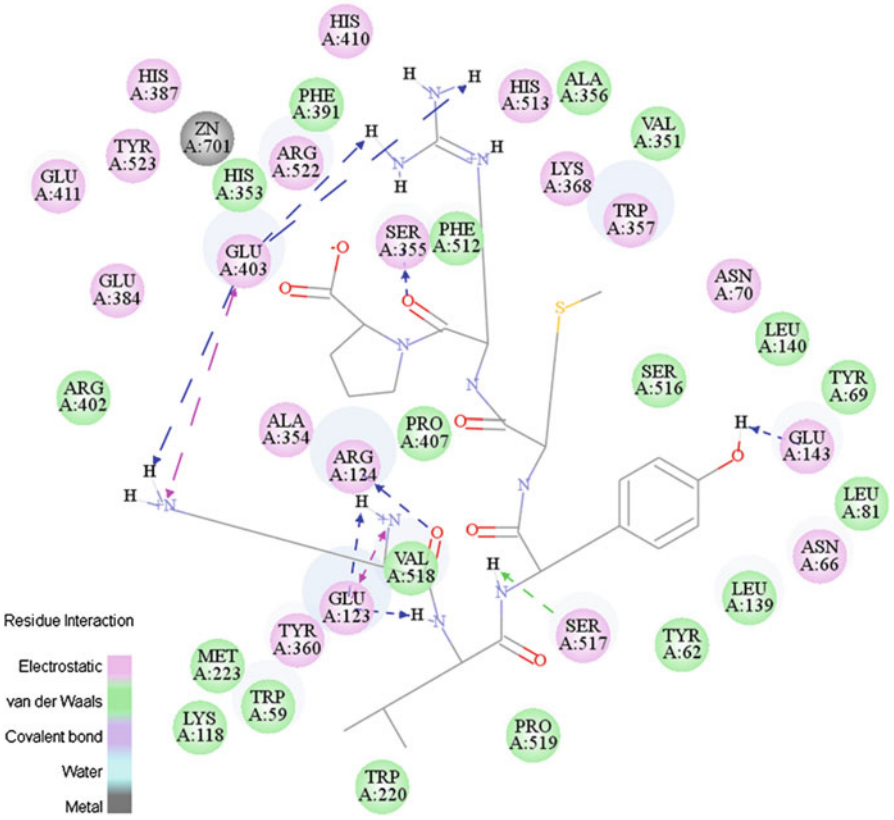

Fig. 9.51 Main interaction forces between oligopeptide KLYMRP and ACE amino acid residues (pH 7.4, 300 K)

KLYMRP was positive, and this may be caused due to the electrostatic repulsion generated by other adjacent groups.

In addition, it was shown from the above table that the metal ions in ACE could strongly interact with oligopeptide KLYMRP, and the distances from Zn ion to O_{119} and O_{120} on KLYMRP were 2.261 Å and 2.314 Å, respectively, which were close to the sum of the covalent radiuses (2.14 Å) of O atom (1.4 Å) and Zn atom (0.74 Å), indicating that the carbonyl at oligopeptide KLYMRP could form a coordination bond with Zn ion (Guo Huiqing et al. 2010). It was also the reason why the interaction between Zn atom and oligopeptide KLYMRP could reach −118.7700 kcal/mol.

It was shown from Fig. 9.52 that Zn ion could form a coordination bond with the carboxyl oxygen atoms (O_{119} and O_{120}) of PRO6 on oligopeptide, and the distance from it to the carboxyl oxygen atoms on 384-bit glutamic acid and 411-bit glutamic acid in ACE was also enough to form the coordination bonds. These three groups and the six coordination bonds formed by Zn ions could stabilize the structure of

Table 9.17 Interaction between oligopeptide KLYMRP and ACE

Action group	Bond length (Å)	Interaction force (kcal/mol)
ACE:ARG124:HH21-O_{24}	2.205	7.7197
ACE:SER355:HG-O_{105}	1.850	−9.6588
H_3-ACE:GLU123:OE2	2.164	−51.1355
H_{26}-ACE:GLU123:OE2	2.434	
H_{45}-ACE:SER517:O	2.498	−4.8263
H_{62}-ACE:GLU143:OE1	1.957	−12.4212
H_{22}-ACE:GLU403:OE1	2.003	−79.6508
H_{100}-ACE:GLU403:OE2	2.049	
H_{103}-ACE:GLU403:OE1	2.013	
H_{103}-ACE:GLU403:OE2	2.146	
ACE:Zn701-O_{119}	2.261	−118.7700
ACE:Zn701-O_{120}	2.314	
ACE:Cl703-O_{113}	16.680	0
ACE:Cl704-O_{35}	4.892	−9.9818

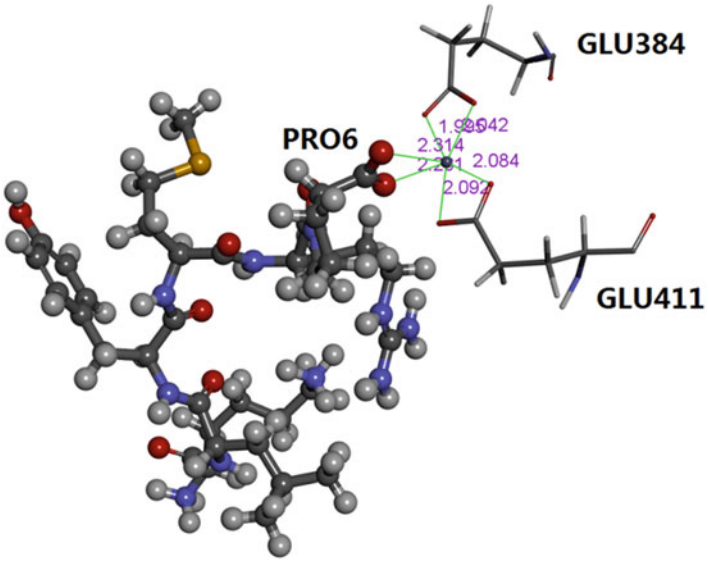

Fig. 9.52 Interaction between Zn ion and amino acid residues

ACE-oligopeptide compound to a large extent, thereby inhibiting ACE activity (Yamamoto et al. 2007).

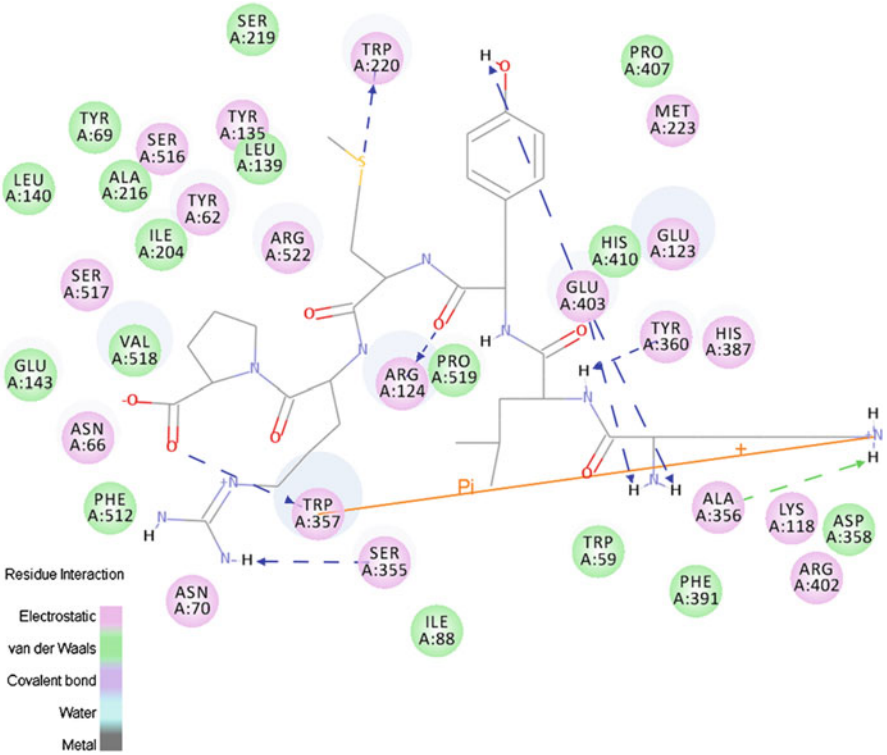

Fig. 9.53 Main interaction force between oligopeptide KLYMRP and ACE amino acid residues (pH 8.4, 300 K)

5.6.3 Stability of Interaction Between Oligopeptide KLYMRP and ACE

As the important factors to impact the interaction between molecules, temperature and pH also have a significant impact on the interaction between oligopeptide KLYMRP and ACE. The DS3.5 molecular simulation software can be used to simulate the molecular docking process at different temperatures and pHs to obtain the optimal docking compound. The interaction between oligopeptide KLYMRP and ACE was analyzed, as shown in Figs. 9.53 and 9.54.

With the increase of pH and temperature, 403-bit glutamic acid and 124-bit arginine on ACE always participated in the interaction between them. Meanwhile, some new groups such as tyrosine, alanine, and aspartic acid could also interact with oligopeptide KLYMRP. Specific bond length and interaction force are shown in Table 9.18. In addition, 357-bit and 220-bit tryptophans in ACE could also form the Pi bond with oligopeptide KLYMRP, and it could play a role in stabilizing their interaction.

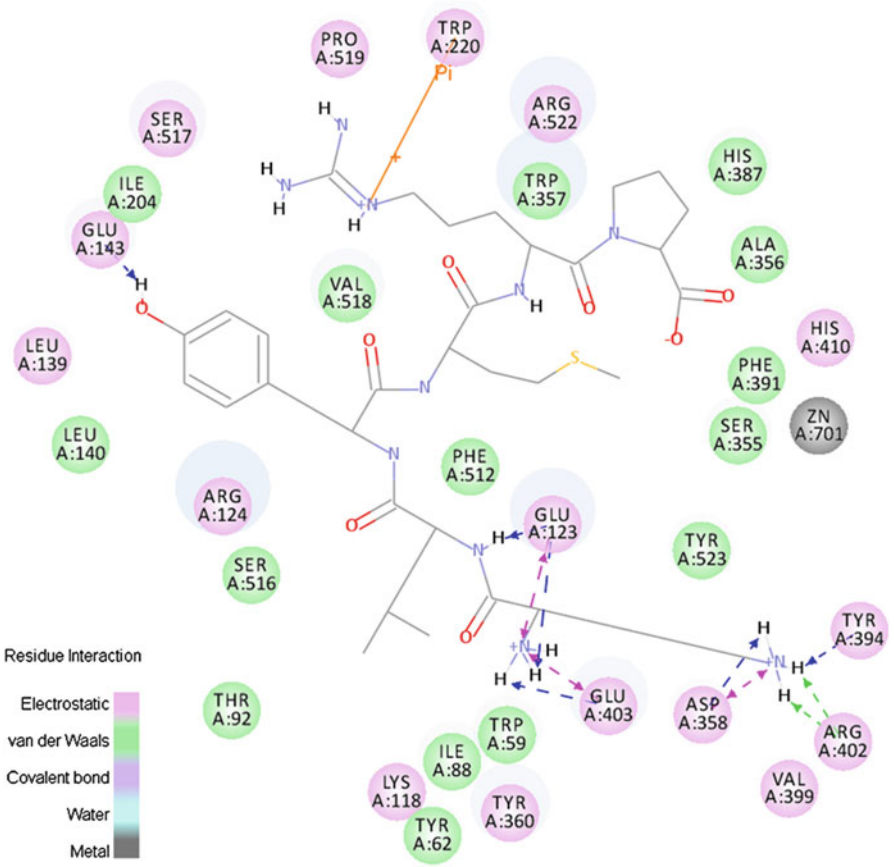

Fig. 9.54 Main interaction force between oligopeptide KLYMRP and ACE amino acid residues (pH 7.4315 K)

In comparison with Tables 9.17 and 9.18, it was shown that the increase in pH and temperature might lead to a decrease in the interaction between the oligopeptide KLYMRP and ACE. As an important residue after the interaction between the two, the interaction force between glutamic acid on ACE and oligopeptide KLYMRP changed from −143.2075 to −28.5356 kcal/mol and −87.8504 kcal/mol, respectively; when pH was 8.4, the interaction force between Zn ion and oligopeptide KLYMRP was positive, indicating that under this condition, there were repulsive forces between Zn ion and some groups on oligopeptide and the interaction was unstable; when the temperature increased, the distance between Zn ion and the sulfur atom on the oligopeptide was 6.070 Å, which was much larger than the sum of the covalent radiuses (2.14 Å) of oxygen atom (1.4 Å) and zinc ion (0.74 Å); the acting force was weak and the interaction was unstable.

Table 9.18 Interaction force between oligopeptide KLYMRP and ACE

Condition	Action group	Bound length (Å)	Interaction force (kcal/mol)
pH 8.4, 300 K	ACE:ARG124:HH21-O_{63}	2.367	−9.9144
	ACE:TRP220:HE1-S_{74}	2.302	−2.0483
	ACE:TRP357:HE1-O_{118}	2.497	−20.3167
	H_2-ACE:GLU403:OE2	2.152	−28.5356
	H_3-ACE:GLU403:OE2	2.434	
	H_{61}-ACE:GLU403:OE1	1.932	
	H_{21}-ACE:ALA356:O	1.816	−12.2489
	H_{25}-ACE:TYR360:OH	2.445	0.0911
	H_{98}-ACE:SER355:OG	2.205	−0.4414
	ACE:Zn701-H_{102}	4.633	23.1370
	ACE:Cl703-H_{98}	19.073	0
	ACE:Cl704-H_{102}	6.614	−2.8376
Ph7.4, 315 K	H_2-ACE:GLU403:OE1	2.488	−38.4605
	H_2-ACE:GLU403:OE2	2.076	
	H_{20}-ACE:ARG402:O	1.830	−7.6691
	H_{21}-ACE:ARG402:O	2.450	
	H_{21}-ACE:TYR394:OH	2.179	−8.6251
	H_{22}-ACE:ASP358:OD2	2.052	−24.4351
	H_3-ACE:GLU123:OE1	2.491	−37.4369
	H_{26}-ACE:GLU123:OE1	1.965	
	H_{62}-ACE:GLU143:OE2	1.870	−11.9530
	ACE:Zn701-H_{78}	3.788	−5.7339
	ACE:Zn701-S_{75}	6.070	
	ACE:Cl703-H_{59}	21.182	0
	ACE:Cl704-H_{94}	4.908	−9.0554

References

Brantl V, Teschemacher H, Henschen A, et al. Novel opioid peptides derived from casein (beta-casomorphins). I. Isolation from bovine casein peptone[J]. Hoppe Seyler's Z Physiol Chem. 1979;360(9):1211.

Byun HG, Kim SK. Purification and characterization of angiotensin I converting enzyme (ACE) inhibitory peptides from Alaska Pollack (Theragra chalcogramma) skin[J]. Process Biochem. 2001;36(12):1155–1162.

Chen Meizhen, Yu Jie, Guo Huimin. Study on the scavenging activity on hydroxyl radical of enzymic hydrolysates of soy protein isolates [J]. Food Sci. 2002;23(1):43–6.

Chen Xiu, Chen Weizhou, Zeng Guiyun. Cardiovascular pharmacology. 3rd Edition[M] ed. People's Health Publishing House: Beijing; 2003. p. 352–3.

Chen HM, Muramoto K, Yamauchi F. Structural analysis of antioxidative peptides from soybean. β-conglycinin [J]. J Agric Food Chem. 1995;43(3):574–8.

Cheung HS, Wang FL, Ondetti MA, et al. Binding of peptide substrates and inhibitors of angiotensin-converting enzyme. Importance of the COOH-terminal dipeptide sequence [J]. J Biol Chem. 1980;255:401–7.

Coakley WT, James CJ. A simple linear transform for the Folin-Lowry protein calibration curve to 1.0 mg/ml. Anal Biochem. 1978;85(1):90–7.

Cushman DW, Cheung HS, Sabo EF, Ondetti MA. Design of potent competitive inhibitors of angiotensin-converting enzyme. Carboxyalkanoyl and mercaptoalkanoyl amino acids. Biochemistry. 2002;16(25):5484–91.

Deng JC. Effect of temperatures on fish alkaline protease, protein Interaction and texture quality. J Food Sci. 1981;46(1):62–5.

Douglas RG, Sturrock ED. Structure-based design of domain-selective angiotensin-converting enzyme inhibitors. Drug Discovery Afr. 2012:355–77.

Dun XP, Chen ZW. Enzyme hydrolysis preparation of rice small polypeptides from rice residue [J]. Food Sci. 2004;25(6):113–6.

Enyonam Quist E, Dixon Phillips R, Saalia FK. Angiotensin converting enzyme inhibitory activity of proteolytic digests of peanut (Arachis hypogaea L.) flour. LWT Food Sci Technol. 2009;42 (3):694–9.

Gill I, López-Fandiño R, Jorba X, et al. Biologically active peptides and enzymatic approaches to their production[J]. Enzym Microb Technol. 1996;18(3):163.

Grimble GK, Silk DBA. Intravenous protein hydrolysates-Time to turn the clock back[J]. Clin Nutr. 1990;9(1):39–45.

Guang C, Phillips RD. Purification, activity and sequence of angiotensin I converting enzyme inhibitory peptide from Alcalase hydrolysate of peanut flour[J]. J Agric Food Chem. 2009;57 (21):10102–6.

Guanhong L. Studies on angiotensin-converting enzyme inhibitory peptides derived from food proteins [D]. Wuxi: Jiangnan University; 2005.

Guangchang P et al. Theoretical basis and prospect of research progress of bioactive peptides[J]. Food Sci. 2001;22(2):80–4.

Guo H. Preparation of wheat germ protein and its antioxidant function[D]. Wuxi: Jiangnan University; 2009.

Guo HQ, Mao H, Zhao B, et al. Molecular mechanism study of targeting of two angiotensin-converting enzyme inhibitory peptides[J]. Food Sci. 2010;31(23):1–5.

Jamdar SN, Rajalakshmi V, Pednekar MD, Juan F, Yardi V, Sharma A. Influence of degree of hydrolysis on functional properties, antioxidant activity and ACE inhibitory activity of peanut protein hydrolysate. Food Chem. 2010;121(1):178–84.

Jianping Wu, Xiaolin Ding. Characterization of inhibition and stability of soy-protein-derived angiotensin I-converting enzyme inhibitory peptides. Food Res Int. 2002;35(4):367–75.

Jung WK, Mendis E, Je JY, et al. Angiotensin I-converting enzyme inhibitory peptide from yellowfin sole (Limanda aspera) frame protein and its antihypertensive effect in spontaneously hypertensive rats [J]. Food Chem. 2006;94(1):26–32.

Kannel WB. Blood pressure as a cardiovascular risk factor: prevention and treatment. JAMA: J Am Med Assoc. 1996;275(20):1571–6.

Liao Dan-kui, Sun Xiu-hua, Wan Shun-gang, Yang Ke-di, Tong Zhang-fa, Liu Xiong-min. Enzymatic Hydrolysis and Screening of Prodrugtype Angiotensin I-converting Enzyme Inhibitor from Chicken Egg Yolk [J]. Fine Chem. 2006;8:757–9.

Liu Lisheng. Hypertension[M]. Beijing: People's Health Publishing House; 2001. p. 30–4.

Liu YD, Cao YP. Prospect review on polypeptide [J]. Food Sci. 2002;23(8):319–20.

Marquez MC, Fernandez V. Enzymic hydrolysis of vegetable proteins: mechanism and kinetics [J]. Process Biochem. 1993;28:481–90.

Mo Qi. A Study on the Papain Hydrolysis of Peanut Meal [J]. Cereal Feed Ind. 1996;12:37–8.

Matsui T, Li C, Osajima Y. Preparation and characterization of novel bioactive peptides responsible for angiotensin I – converting enzyme inhibition from wheat germ [J]. J Peptide Sci. 1999;5(7):289–97.

Munilla-moran R, Saborido-rey F. Digestive enzymes in marine species. 1: Protease activities ingut from redfish (Sebastes mentella), seabream (Sparusaarata) and turbot (Scophthalmus inaximus) [J]. Comp Biochem Physiol B: Biochem Mol Biol. 1996;113(2):395–402.

Nakagomi K, Fujimura A, Ebisu H, et al. Acein-1, a novel angiotensin-I-converting enzyme inhibitory peptide isolated from tryptic hydrolysate of human plasma[J]. FEBS Lett. 1998;438(3):255–7.

Ondetti MA, Cushman DW. Design of specific inhibitors of angiotensin-converting enzyme: new class of orally active antihypertensive agents [J]. Science. 1977;196(4288):441–4.

Patchett AA, Harris E, Tristram EW, et al. A new class of angiotensin-converting enzyme inhibitors [J]. Nature. 1980;298:280–3.

Shen Beiying. Study on Antioxidant Peptides of Soybean Protein [J]. Chinese fats oils. 1996; 21(6):21–4.

Stevens RL, Micalizzi ER, Fessler DC, Pals DT. Angiotensin I converting enzyme of calf lung. Method of assay and partial purification. Biochemistry. 2002;11(16):2999–3007.

Rohrbach MS, Williams JEB, Rolstad RA, et al. Purification and substrate specificity of bovine angiotensin-converting enzyme [J]. J Biol Chem. 1981;256:225–30.

Ruiz JÁG, Ramos M, Recio I. Angiotensin converting enzyme-inhibitory activity of peptides isolated from Manchego cheese. Stability under simulated gastrointestinal digestion[J]. Int Dairy J. 2004;14(12):1075–80.

Saito Y, Wanezaki K, Kawato A, et al. Structure and activity of angiotensin I converting enzyme inhibitory peptides from sake and sake lees [J]. Biosci Biotechnol Biochem. 1994;58(10):1767–71.

Sheng GH. Function and application of soybean peptide [J]. Food Sci Technol. 1993;6:21–6.

Tello PG. Enzymatic hydrolysis of whey protein: I kinetic models [J]. Biotechnol Bioeng. 1994;44:523–8.

Vermeirssen V, Deplancke B, Tappenden KA, Van Camp J, Gaskins HR, Verstraete W. Intestinal transport of the lactokinin Ala-Leu-Pro-Met-His-Ile-Arg through a Caco-2 Bbe monolayer. J Pept Sci. 2002;8(3):95–100.

Wang Jiazheng. Protein technical handbook[M]. Beijing: Science Press; 2002.

Wang M, Gu WY. On preparation of enzyme-modified peptides from maize gluten meal [J]. Sci Technol Cereal Oils Foods. 1999;1–3.

Wang H, Ng TB. Pleureryn, a novel protease from fresh fruiting bodies of the edible mushroom Pleurotus eryngii. Biochem Biophys Res Commun. 2001;289(3):750–5.

Wang Q, Wang CY, Hu H, et al. Structural characterization and structure-activity relationship of ACE inhibitory peptides from peanut [J]. Food Sci. 2013.

Wu JP, Ding XL. Characterization of inhibition and stability of soy-protein-derived angiotensin I-converting enzyme inhibitory peptides[J]. Food Res Int. 2002;35:367–75.

Yamamoto D, Takai S, Miyazaki M. Prediction of interaction mode between a typical ACE inhibitor and MMP-9 active site. Biochem Biophys Res Commun. 2007;354(4):981–4.

Yude L, Yanping C. Development of biological protein peptide[J]. Food Sci. 2002;23(8):319–20.

Zhang XH. Preparation of soy peptide and study on the separation of purified grade [D]. Guangzhou: South China University of Technology; 2002.

Zhang YH. Study on preparation of peanut oligopeptides and its functional activities [D]. Beijing: Chinese Academy of Agricultural Sciences; 2007.

Zhang XS, Feng JC. Study on protease production of functional protein short peptides [J]. Anim Sci Vet Med. 2004;21(3):48–51.

Zhang YH, Wang Q. Peanut protein hydrolyzing by Alcalase to prepare peanut oligopeptides [J]. Trans CSAE. 2007;23(4):258–63.